

THE UNIVERSITY OF CALGARY

ELECTROMAGNETIC FIELD EFFECTS ON
WATER-IN-OIL EMULSION

by

ILICE S.L. TAN

A THESIS

SUBMITTED TO THE FACULTY OF GRADUATE STUDIES
IN PARTIAL FULFILLMENT OF THE REQUIREMENTS FOR THE
DEGREE OF MASTER OF SCIENCE

DEPARTMENT OF ELECTRICAL ENGINEERING

CALGARY, ALBERTA

March, 1987

© Illice S.L. Tan 1987

Permission has been granted to the National Library of Canada to microfilm this thesis and to lend or sell copies of the film.

The author (copyright owner) has reserved other publication rights, and neither the thesis nor extensive extracts from it may be printed or otherwise reproduced without his/her written permission.

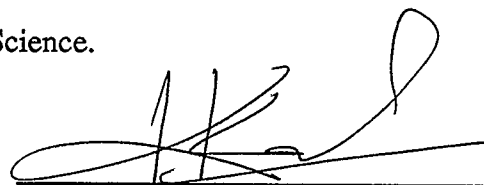
L'autorisation a été accordée à la Bibliothèque nationale du Canada de microfilmer cette thèse et de prêter ou de vendre des exemplaires du film.

L'auteur (titulaire du droit d'auteur) se réserve les autres droits de publication; ni la thèse ni de longs extraits de celle-ci ne doivent être imprimés ou autrement reproduits sans son autorisation écrite.

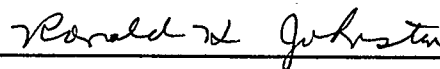
ISBN 0-315-35970-6

THE UNIVERSITY OF CALGARY
FACULTY OF GRADUATE STUDIES

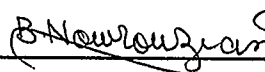
The undersigned certify that they have read, and recommend to the Faculty of Graduate Studies for acceptance, a thesis entitled "*Electromagnetic Field Effects on Water-In-Oil Emulsion*" submitted by Ilice S.L. Tan in partial fulfillment of the requirements for the degree of Master of Science.



Supervisor, Dr. K.V.I.S. Kaler
Dept. of Electrical Engineering



Dr. R.H. Johnston
Dept. of Electrical Engineering



Dr. B. Nowrouzian
Dept. of Electrical Engineering



Dr. R.G. Moore
Dept. of Chemical Engineering

Date 30th March 87.

ABSTRACT

The physical effect of an electromagnetic field on an oil-field water-in-oil (w/o) emulsion is studied over the frequency range of 10 MHz to 500 MHz. A wire-wire electrode configuration built into an observation chamber was used to produce the required non-uniform electric field. The spacing between the two wires was 0.165mm and the applied voltage across the electrodes was 10 Vrms.

The water droplets are found to collect, in the form of chains, at the electrode surfaces throughout the frequencies investigated. The optimum frequency for such a collection within the above frequency range is approximately 450 MHz. These results may be applied to separate the dispersed water from the oil in w/o emulsions. Other physical effects observable throughout the same frequency range include : (1) orientation of the agglomerate droplets, (2) mutual attraction between droplets, (3) "pearl chain" formation, and (4) droplet coalescence.

ACKNOWLEDGEMENTS

The author would like to thank her supervisor, Dr. Karan Kaler, for his helpful discussions, and especially in the final write up of the thesis.

Many thanks are due to Mdm. Teh Chew Eng (the author's mother), Dr. D.C. Cooper, and Mr. Dennis Wong for their morale support, love, and encouragement. The author expresses her sincere gratitude to Ella Lok for typing the thesis.

The financial support provided by the Department of Electrical Engineering is also greatly appreciated.

To the Glory of

God.

His guidance, wisdom, and grace

He abundantly gives.

TABLE OF CONTENTS

Table of Contents	vi
List of Tables	viii
List of Figures	ix
List of Symbols	x
1. INTRODUCTION.	1
1.1. Research Application	1
1.2. Objective of the Thesis	2
1.3. Summary of the Thesis	3
2. LITERATURE REVIEW.	4
2.1. Effects of Electric Field on Dispersed Systems	4
2.2. Dielectric Properties of W/O Emulsion	12
3. THEORY ON FIELD EFFECTS ON DISPERSED SYSTEMS.	14
3.1. Introduction	14
3.2. Electric and Magnetic Properties	16
3.3. Dielectric Polarization	19
3.4. Polarization Mechanisms	24
3.5. Dispersion in a Dispersed System	28
3.6. Physical Effects on Dispersed Droplets	30
3.6.1. Orientation	30
3.6.2. Mutual Dielectrophoresis	31
3.6.3. "Pearl Chain" Formation	33
3.6.4. Droplet Coalescence	34
3.6.5. Dielectrophoresis (DEP)	34
3.7. Techniques Used in the Present Studies	40
4. EXPERIMENTAL.	44
4.1. Experimental Requirements	44
4.2. Experimental Setup and Apparatus	47
4.2.1. The Chamber	49

4.2.2. The Directional Couplers Used	51
4.2.3. The W/O Emulsion Used	54
4.3. Experimental Procedures	54
4.3.1. Part 1 : Physical Behaviour of the Emulsion	55
4.3.2. Part 2 : Optimum Frequency for Droplet Collection	55
5. RESULTS AND DISCUSSION.	58
5.1. Part 1 : Physical Behaviour of the Emulsion	58
5.2. Part 2 : Optimum Frequency for Droplet Collection	67
6. CONCLUSIONS AND RECOMMENDATIONS.	75
REFERENCES	77

LIST OF TABLES

3.1. Various dispersed systems and corresponding particle diameters	15
3.2. Characteristics of various polarization mechanisms	25
4.1. Coupling factor of NMC-3041-20 directional coupler	53
5.1. Measured and calculated average velocities at 450 MHz	72

LIST OF FIGURES

2.1. Physical effects observable in dispersed systems	5
3.1. Electromagnetic spectrum	17
3.2. Dielectric polarization	20
3.3. Resonance dispersion in dielectric media	23
3.4. Relaxation dispersion in dielectric media	23
3.5. Dielectric dispersions of various polarization mechanisms	26
3.6. Orientation of an electric dipole	31
3.7. Mutual dielectrophoresis	32
3.8. Uniform field (parallel plates electrode configuration)	35
3.9. Non-uniform field (pin-plate electrode configuration)	35
3.10. Collection of "pearl chains" at the electrodes	37
3.11. Interpretation of yield spectrum	39
3.12. Forces on a droplet in a non-uniform field	42
4.1. Various electrode shapes for producing dielectrophoretic fields	45
4.2. Theoretical setup	46
4.3. Return loss of the load	46
4.4. Experimental setup for studying field effects on w/o emulsion	48
4.5. The Chamber	50
4.6. Coupling factor of SEC-145z directional coupler	52
4.7. Voltage at the load	53
4.8. The distance travelled by the droplet	57
5.1. Effect of electric field on w/o emulsion	59
5.2. Orientation of agglomerate droplets	60
5.3. Mutual attraction between droplets.	61
5.4. Orientation of mutual attracted droplets	62
5.5. Spontaneous droplet coalescence	62
5.6. Pearl chain" formation	64
5.7. Electric field distribution in a wire-wire electrode configuration	65
5.8. Chains of droplets collected at the electrodes	66
5.9. Velocity spectra of water droplets	68
5.10. Normalised velocity spectrum of 5.1 μm water droplets	70

LIST OF SYMBOLS

OPERATORS

∇	gradient operator
$ \quad $	magnitude
j	$\sqrt{-1}$
$\text{Re } \{x\}$	real part of complex number x
$\text{Im } \{x\}$	imaginary part of complex number x

VARIABLES

a	droplet radius
d	distance between two electrodes
e	counterion charge
D_c	mean diffusion coefficient of counterions
\vec{D}	electric flux density
\vec{E}	electric field
\vec{E}_{local}	local electric field
\vec{E}_{chain}	threshold field strength for "pearl chain" formation
f	external field frequency
f_r	relaxation frequency
f_{res}	resonant frequency
\vec{F}	force
\vec{F}_{drag}	drag force
\vec{F}_D	dielectrophoretic force
k	Boltzmann constant
K	a proportionality constant
K_e	effective excess permittivity
N	number of electric dipoles
\vec{P}	polarization vector
q	positive or negative charge
T	absolute temperature
\vec{v}	droplet velocity
ϵ^*	complex permittivity of a material
ϵ'	$\text{Re } \{\epsilon^*\}$, dielectric permittivity of a material
ϵ''	$\text{Im } \{\epsilon^*\}$, dielectric loss factor of a material

ϵ_0	dielectric constant of free space
ϵ_c^*	complex permittivity of continuous phase
ϵ_d	complex permittivity of dispersed phase
η	viscosity of continuous phase
κ^*	relative complex permittivity of a material
κ'	relative dielectric permittivity of a material
κ''	relative dielectric loss factor of a material
κ_m'	$\text{Re} \{\kappa^*\}$, relative magnetic permeability of a material
κ_m''	$\text{Im} \{\kappa^*\}$, relative magnetic loss factor of a material
$\Delta\kappa$	dielectric increment
μ	mobility of the counterions
μ^*	complex permeability of a material
μ'	$\text{Re} \{\mu^*\}$, magnetic permeability of a material
μ''	$\text{Im} \{\mu^*\}$, magnetic loss factor of a material
μ_0	free space magnetic permeability
$\bar{\mu}_e$	average electric dipole moment
μ_e	electric dipole moment
ϕ	volume fraction of dispersed phase
ω	angular frequency
ψ	potential at the outer Helmholtz plane
ρ_s	surface charge density at the double layer
σ	conductivity of a material
τ	relaxation time
ξ	connecting line through a particle centre
ζ	zeta potential

CHAPTER 1

INTRODUCTION

1.1. Research Application

Crude-petroleum obtained from the well bores often appears in the form of an emulsion. An emulsion is a system comprising of one liquid phase dispersed in another liquid phase in the form of droplets. In general, the emulsions from well bores may be in the form of water dispersed in oil (w/o) or oil dispersed in water (o/w) [1]. However, the present research is focused on w/o emulsions only.

Oil-field emulsions must have the major part of their water removed, before further petroleum processing. The reason being the mineral salts which are present in the water phase tend to deposit on the refinery equipment, plug the pipelines, and cause corrosion in both [2, 3].

In general, dispersed water droplets settle due to gravity and eventually *phase separation* (complete separation of the two phases) is achieved; however, this process is rather time consuming [1]. At the present state of the art, a number of methods are commercially utilized to speed up phase separation. These include the use of demulsifiers, heat, as well as electric field [2, 1]. These methods aid the process of gravity separation either by enhancing droplet coalescence or by reducing the viscosity of the oil [2, 3, 4, 1].

Although electric field phase separation techniques have already been utilized, extensive research has only been carried out in the low end (i.e. < 1 MHz) of the frequency spectrum [1,5,6,7,8,9,10,11,12]. In fact, the presently available electrical separators operate using field frequencies at or below 60 Hz [13,1]. These include the vertical grid electrostatic treater (HTI Superior) and the dual polarity electrostatic treater (C-E Natco Combustion Engineering). In the low end of the frequency spectrum, the range of 50 Hz to 60 Hz was found to be the optimum frequencies for droplet coalescence [4,8]. Not much research, however, has been carried out in the use of higher frequency electric fields. The investigation of the use of higher frequency fields is important in order to assess their use in phase separation.

1.2. Objective of the Thesis

The principle objective of the present work is to investigate the possibility of using high frequency electromagnetic fields in phase separation. This investigation is carried out in the frequency range of 10 MHz to 500 MHz. The work first addresses the physical effects of high frequency electromagnetic fields on a sample w/o emulsion. The effect most pertinent to phase separation (in this case collection of droplets at the electrode surfaces) is further studied in the same frequency range to determine the optimum frequency (or possibly range of frequencies).

The physical effects of high frequency fields in the investigations are observed with the aid of an optical microscope. The visual observations are also recorded on video tapes to provide a permanent record. A wire-wire electrode configuration, as shown in Figure 4.1, is used to generate the non-uniform electric field within the emulsion. The reason for using non-uniform fields is discussed in section 3.7. A voltage of 10 Vrms is applied across the two electrodes spaced 0.165 mm apart.

1.3. Summary of the Thesis

Chapter 2 provides a literature review of the physical effects of the electromagnetic fields on various dispersed systems, and on the dielectric properties of w/o emulsions. Chapter 3 deals with the development of theory for the behaviour of the w/o emulsion. Chapter 4 describes the experimental setup and procedures used in this investigation. This is followed by Chapter 5 which contains the experimental findings, and a discussion of the results. The conclusions and recommendations for further research are presented in Chapter 6.

CHAPTER 2

LITERATURE REVIEW

2.1. Effects of Electric Field on Dispersed Systems

A literature survey has indicated that very little research has been carried out on the effect of higher frequency electric fields (i.e. > 10 MHz) on the oil-field water-in-oil (w/o) emulsions. Thus example systems are examined in this frequency range to determine the nature of various physical effects that may arise in w/o emulsions.

Numerous physical effects have already been observed when other dispersed systems are exposed to electric fields. See Figure 2.1. These include dispersed particles exhibiting oscillatory motion, deformation, orientation with their long axes aligned perpendicular or parallel to the electric field lines, mutual attraction, coalescence/fusion, "pearl chain" formation, gross translational motion (i.e. dielectrophoresis), and re-emulsification/destruction. These physical effects are discussed in detail in the following section.

Oscillatory Motion of Dispersed Particles

Oscillatory motion of dispersed particles arises due to electrophoresis as discussed in section 3.6.5, and is observable at low electric field frequencies (i.e. $\approx < 100$ Hz). In this study only high frequency field effects are explored, in which case particle oscillation due to electrophoresis is not observable.

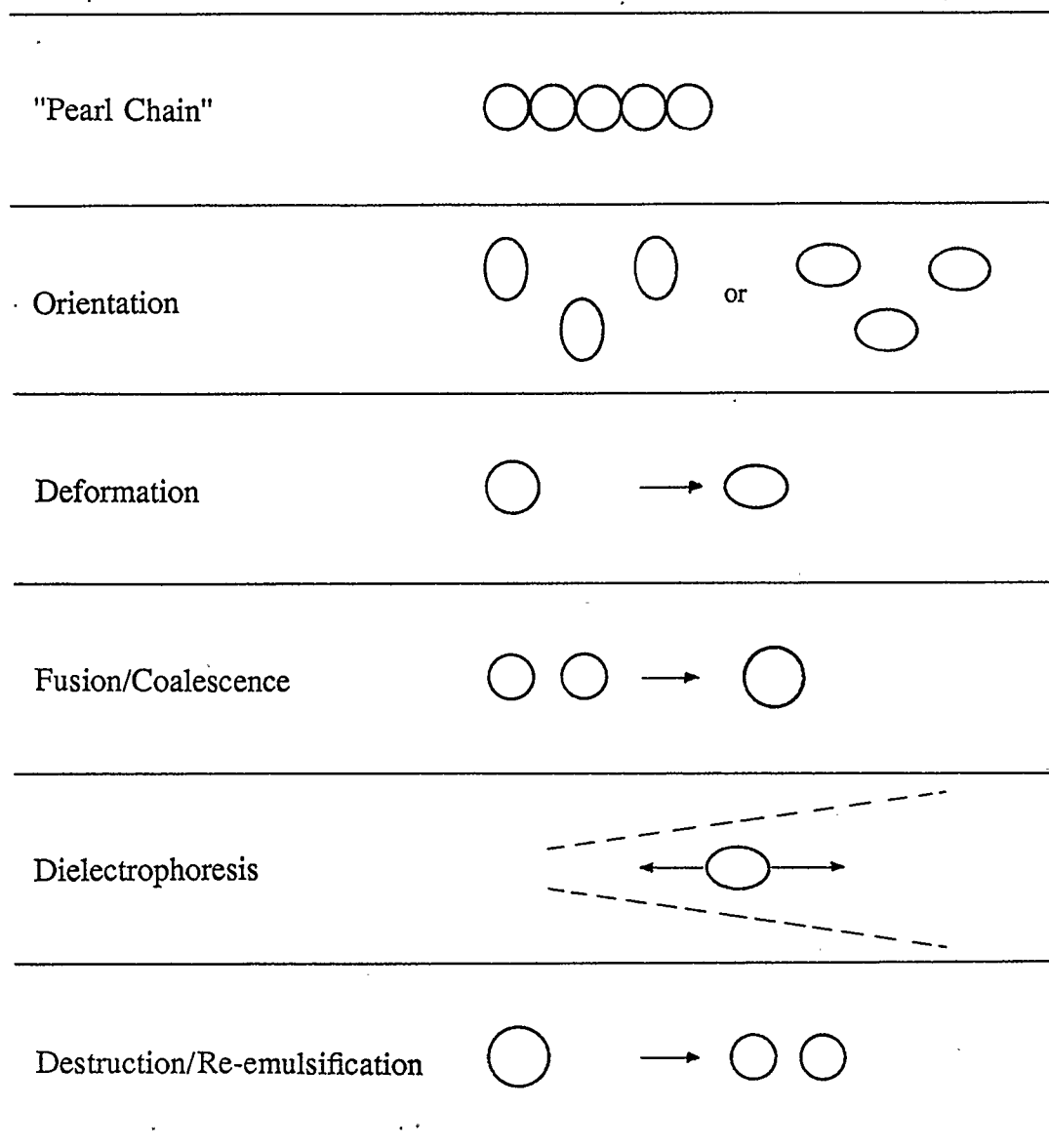


Figure 2.1. Physical effects observable in dispersed systems [14].

Particle Deformation

Particle deformation has been found to occur when non-rigid dispersed particles, like water droplets, are exposed to electric fields [1, 13, 15]. Such deformation has been reported by Panchenkov *et. al.* [8] and Babalyan *et. al.* [16] for water droplets dispersed in oil. The spherical water droplets were deformed into ellipsoids. The frequencies of electric fields used in these cases were between 50 Hz to 382 kHz. A spherical droplet elongates as a result of positive and negative charges within the droplet being attracted towards the oppositely charged electrodes [1, 3, 4]. As the frequency of the electric field increases, the migration of charges within the droplet will not be able to follow the change in the direction of the applied field; in this case the deformation of the droplet will be negligible. In the present study, the emulsion is exposed to frequencies in the range of 10 MHz to 500 MHz and hence, droplet deformation is not expected to be observable.

Particle Orientation

The alignment of the dispersed particles with their long axes *perpendicular* to the electric field lines has so far only been observed in living cells [17, 18, 19]. This is because living cells comprise several differing regions of dielectrics and are non-spherical [19]. In fact, Teixeira-Pinto *et. al.* [19] have concluded that no asymmetric non-viable matter exhibits orientation effects with its long axis perpendicular to the field lines. Hence, such an orientation is not expected to occur in a w/o emulsion system.

Teixeira-Pinto *et. al.* [20], in studying the electric field effects on starch particles in the frequency of 0.1 MHz to 100 MHz, observed that the asymmetric starch particles orientated with their long axes along the uniform electric field lines. According to Teixeira-Pinto *et. al.*, symmetric spheres should have no preferential orientation since they have no long axes. However, in w/o emulsions some droplets are dispersed in the form of aggregates. In such a case, a group of droplets will appear as an asymmetric particle as a whole. Under this situation, orientation effects may manifest themselves in the present investigation.

Coalescence/Fusion

Panchenkov *et. al.* [8] observed mutual attraction of water droplets followed by droplet coalescence in a w/o emulsion. The emulsion was under the influence of a uniform electric field intensity of 3 kV/cm, and in the frequency range of 50 Hz to 382 kHz. They attributed the phenomenon of mutual attraction to the polarization of water droplets when exposed to an externally applied field. As a result, each water droplet acted as a dipole and they attracted each other [3, 12, 13, 15]. Such dipole-dipole attraction also induced collision and enhanced droplet coalescence [3, 12, 13, 15].

Pohl [17] attributes the dipole-dipole attraction to the presence of electric field non-uniformities around each suspended particle that differs in dielectric properties from the suspending medium. The individual particle then experiences a field gradient near each other, and is therefore attracted to the higher field intensity

regions near each other. Pohl refers to such an attraction and the resulting motion as mutual dielectrophoresis.

"Pearl Chain" Formation

"Pearl chain" formation is one of the early observations when dispersed systems were exposed to high frequency electric fields. This was observed as stringing of fat particles of an emulsion (See Pohl [17]) along the uniform electric field lines. A similar observation has also been reported for the suspension of polystyrene spheres and starch particles when exposed to uniform electric fields of frequencies between 0.1 MHz to 100 MHz [19]. Pohl and Crane [21] studied the response of yeast cells to a non-uniform electric field in the frequency range of 100 Hz to 100 MHz. They also observed the cells attached to the electrodes in a chain-like formation.

Chain formation in w/o emulsions, however, has only been observed for low frequencies. Joo *et. al.* [22] subjected an emulsion prepared from silicone oil and deionized water to a uniform 60 Hz electric field. The chaining of the water droplets was observed after the field had been applied for 12 hours. The emulsion was subjected to four different field intensities ranging from 52 kV/m to 520 kV/m. The concentration of the water in volume fractions ranged between 0.001 to 0.1. Babalyan *et. al.* [16] also observed chain formation when 50 Hz to 60 Hz uniform electric fields were applied to the w/o emulsions of 0.05 to 0.2 volume fractions of water. Electric field strengths of 3 kV/cm and 5 kV/cm were used in their investigations.

The formation of a chain of dispersed particles [17,21,23] is the result of the end-to-end attachment of particles, similar to the chaining of particles, due to mutual attraction. Hence, Pohl refers to such behaviour as the "pearl chain" formation and attributes it to the effect of mutual dielectrophoresis [17].

Recently, Sauer [24,25] has theoretically investigated the nature of the interacting force between two rigid spheres of the same size and dielectric constant under the influence of an applied electromagnetic field. His investigation concludes that the interacting force is dependent on the angle and the position of the particles with respect to each other and the electric field line. Although no general closed form solution could be obtained for the interacting force, Sauer presented the solution for three special cases: (1) ξ is parallel to the field lines, (2) ξ is perpendicular to the field lines, and (3) particles are on a 2-dimensional plane, where ξ is the line connecting the particle centres. The solution for (1) indicates that the interacting force is attractive, while the solution for (2) indicates that the force is repulsive. The solution for (3) indicates that the relative motion of the two particles is an incomplete elliptical trajectory. His derivation is based on a dilute suspension whereby hydrodynamic interaction between the particles can be neglected. Both the suspending medium and suspended particles exhibited dielectric loss. The electric field was assumed to be uniform, while the magnetic field effects were neglected. Although Sauer's results are based on rigid spherical particles, they are equally valid for spherical water droplets at very high frequency where droplet deformation is minimal.

Dielectrophoresis

Movement of the dispersed particles to the region of higher electric field intensity has been observed by Pohl and Crane [21]. They have observed chains of yeast cells collecting at the two pin electrodes (regions of highest field intensity) when the cell suspension was exposed to non-uniform electric fields. Such a phenomena arises due to the non-uniformities of the applied electric fields and is attributed to dielectrophoresis by Pohl [21,18]. The concentration of the cell suspension used was 2×10^6 cells/ml. The collection rate, that is the number of cells in a chain per defined time, is known to be dependent on the particle concentration, applied voltage, suspension conductivity, and frequency of the applied field [21,18]. It varies linearly with the particle concentration and moderate applied voltages (i.e. < 30 Vrms for pin-pin or wire-wire electrode with electrode spacing of 0.2 mm to 2 mm [18]). At higher voltages, the collection rate deviates from linearity due to heating and stirring effects which disrupt particle collection [21,18]. The collection rate, however, is a complicated function of the suspension conductivity, and frequency of the applied field [18].

Re-emulsification/Destruction

Under the influence of electric fields, dispersed water droplets can also be re-emulsified. Three conditions which prevent droplet re-emulsification have been given by several investigators [12,3,11]. These are : (1) $aE^2 < 0.182 \frac{\gamma}{\epsilon_c}$, (2)

$q < 8 \pi \sqrt{\epsilon_c \gamma a^3}$, and (3) $2\rho_c a |\vec{v}|^2 / \gamma < 13$, where a is the droplet radius, E is the electric field strength, γ is the interfacial tension of the droplet, ϵ_c is the dielectric permittivity of the continuous phase, \vec{v} is the droplet velocity, ρ_c is the density of the continuous phase, and q is the droplet charge. The conditions in (1) and (2) are electrostatic in nature because they imply that for re-emulsification to occur, the cohesive effect of interfacial tension must be overcome by the disruptive electrostatic stress. On the other hand, the condition in (3) is hydrodynamic in nature since for re-emulsification to occur the hydrostatic inertial force should exceed the cohesive effect of interfacial tension. For such condition to exist, the droplets must have been driven sufficiently fast by dielectrophoresis [12].

In summary, electrophoresis, droplet deformation, as well as the orientation of dispersed particles with their long axes perpendicular to the electric field lines will not be observable in the present study. The remaining physical effects, mainly the orientation of the agglomerated droplets with their long axes parallel to the electric field lines, mutual dielectrophoresis, droplet coalescence, "pearl chain" formation, and dielectrophoresis will be observable in present study. All conditions for re-emulsification should also be taken into consideration in deciding the magnitude of the electric field used.

2.2. Dielectric Properties of W/O Emulsion

Physical effects observed in dispersed systems have been known to be a manifestation of the dielectric polarization [26,27]. It is believed that when the field frequency is in the region of the dielectric dispersion of the w/o emulsion, the interaction between the electric field and the emulsion leads to either an intense thermal or hydrodynamic process [26]. For these reasons, it is worthwhile to study the dielectric properties of the w/o emulsions. F.L. Sayakhov and V.S. Khakimov [27] studied the dielectric properties of w/o emulsions in the frequency range of 60 kHz to 25 GHz. They have observed two relaxational dispersions. The first dispersion was between 1 MHz to 10 MHz, while the second was close to 20 GHz. In the same study, the dielectric properties of varying fractions of crude oil were found to show similar dispersion between 1 MHz to 10 MHz, and dehydrated crude oil did not show a dispersion around 20 GHz. Based on these results, they attribute the first dispersion observed in the w/o emulsions to the relaxation of the polar components of the heavy crude adsorbed at the droplet envelopes, and the second dispersion to the relaxation of the polar water droplets. Examples of these polar components adsorbed at the droplet envelopes are asphaltenes and resins [27,28]. The emulsions were prepared with crude oil and distilled water. Three emulsions of 10%, 15%, and 20% water content were used. They claim that such dispersions lower the aggregate emulsion stability and aid in the breaking of the emulsion.

In a later study, which was based on their previous work [27], Sayakhov *et. al.* measured the quantity of the settled water over a frequency range of 2 MHz to 5

MHz [26]. Their results indicated that the optimum frequency for breaking the w/o emulsions is approximately 3 MHz. According to Sayakhov *et. al.*, the optimum frequency is the relaxation frequency of the polar components of the crude oil adsorbed at the droplet envelopes. At the optimum frequency, the electric field is believed to have the greatest effect on the droplet envelopes. This effect together with the absorbed heat weaken the droplet envelopes which aid in the breaking of the emulsions. The emulsions used were prepared using tap water, in volume fractions of 10% and 20%, and crude oil from Arlansk and Sergeyevsk oil-field of Kashkirian ASSR. The study was performed with a microelectrodehydrator. The electric field used was uniform and had a strength of 750 V/cm.

In summary, the physical effects observed when an electric field acts on an emulsion are associated with the frequency of the applied electric field. In addition, there are certain field frequencies at which such effects reach a maximum. These frequencies are the relaxation/resonance frequencies of the polarization mechanisms active in the emulsion systems, and can be determined from the dielectric properties of the system.

CHAPTER 3

THEORY ON FIELD EFFECTS ON DISPERSED SYSTEMS

3.1. Introduction

A *dispersed system* is a system consisting of particles (solid, liquid, or gaseous) dispersed in another medium (solid, liquid, or gaseous) [29]. Examples of dispersed systems are emulsions, milk, and protein solutions. The classification of various dispersed systems, based on the size of dispersed particles, into coarse and colloidal dispersed systems is shown in Table 3.1. Note that the particle diameter of a coarse dispersed system is approximately greater than 1 μm , while the particle diameter for a colloidal dispersed system lies approximately between 10 nm to 1 μm .

An *emulsion* is a heterogeneous system consisting of at least one immiscible liquid dispersed in another in the form of droplets [31]. In general, the diameters of the droplets exceed 0.1 μm . In a simple emulsion, consisting of two phases, the phase which is present in the form of droplets is known as the *discontinuous phase* or *dispersed phase (dispersed droplet)*; while the phase in which the droplets are suspended is known as the *continuous phase* or *suspending medium*.

The effect of electromagnetic fields on a dispersed system is influenced by both the bulk and the interfacial electric and magnetic properties of the dispersed particles and the suspending medium [17, 32, 33, 34]. The electric and magnetic properties of a material are discussed in section 3.2. An electric field whose frequency lies in the

	Range of dimensons	State of dispersions	Examples
Optical microscope	$10^{-1} \text{ cm (1 mm)}$	Coarse	Frog's egg
	$10^{-2} \text{ cm (100 } \mu\text{)}$		Potato starch
			Coarse pigments Coarse emulsions
	$10^{-3} \text{ cm (10 } \mu\text{)}$		Red blood cells Milk
Electron microscope	$10^{-4} \text{ cm (1 } \mu\text{m)}$	Colloidal	Average bacteria Fine emulsions Colloid gold particles
	10^{-5} (100 nm)		
	$10^{-6} \text{ cm (10 nm)}$		High polymer molecules Colloidal carbon black Micelles in solubilized systems
	10^{-7} cm (1n)	Molecular	Protein molecules Thickness of lecithin bi-molecular films
		Atoms	Organic solvent molecules Water molecules
	$10^{-8} \text{ cm (1\AA)}$		

Table 3.1. Various dispersed systems and corresponding particle diameters [30].

range of 3×10^3 Hz to 3×10^{18} Hz, as shown in Figure 3.1 [35], is called an *electromagnetic field*.

3.2. Electric and Magnetic Properties

The *electric* and *magnetic* properties of real materials are described by the complex permittivity (ϵ^*) and the complex permeability (μ^*), respectively [36]. The *dielectric properties* (*complex permittivity*) which describe the interaction of the electric field with the material can be written as

$$\epsilon^* = \epsilon' - j\epsilon'' = \epsilon_0(\kappa' - j\kappa'') = \epsilon_0\kappa^* \quad (3.1)$$

or

$$\epsilon^* = \epsilon' - j\frac{\sigma}{\omega} \quad (3.2)$$

where ϵ' , the *dielectric permittivity*, is a measure of the material's ability to store the electric field energy; ϵ'' , the *total dielectric loss factor*, describes the electrical energy dissipated in the material; κ' , κ'' , and κ^* are the *relative* values of ϵ' , ϵ'' , and ϵ^* with respect to the *permittivity of the free space*, ϵ_0 , respectively; σ is the *material conductivity*, consisting of the static/d.c. conductivity and the conductivity due to dielectric loss; and ω is the angular frequency of the applied field.

Similarly, the *complex permeability* which describes the interaction of the magnetic field with the material can be written as

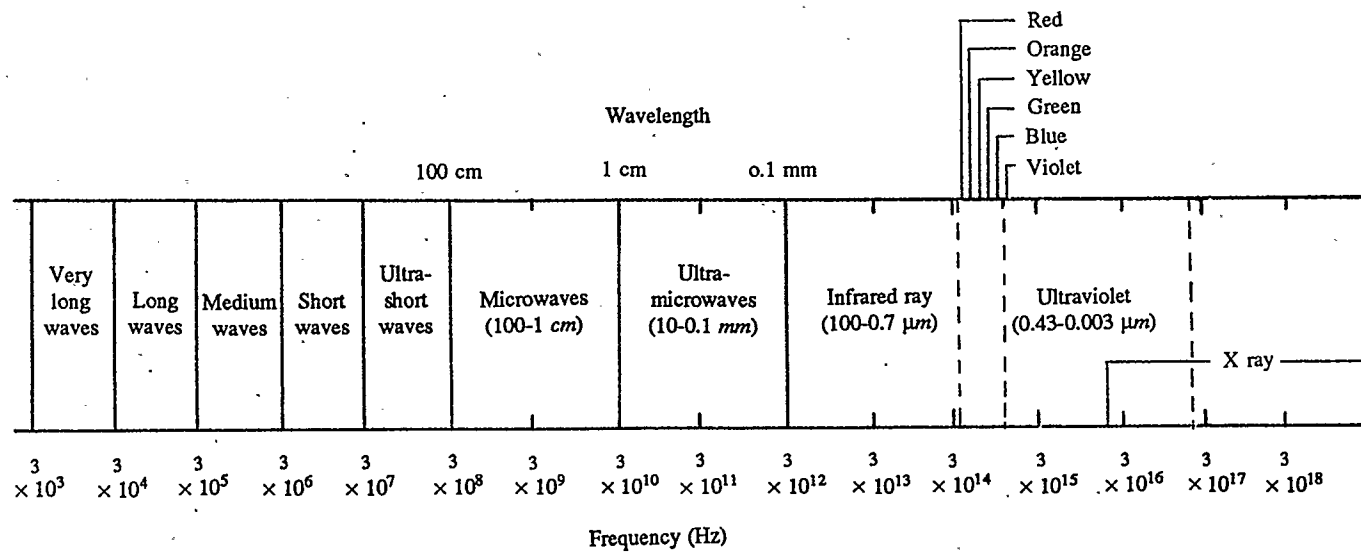


Figure 3.1. Electromagnetic spectrum .

$$\mu^* = \mu' - j\mu'' = \mu_o(\kappa'_m - j\kappa''_m) \quad (3.3)$$

where μ' is a measure of the material's ability to store the magnetic field energy, μ'' describes the magnetic energy dissipated in the material, κ'_m and κ''_m are the *relative* values of μ' and μ'' with respect to the *permeability of the free space*, μ_o , *respectively*.

For effective phase separation using electromagnetic fields, it is desirable to have a large difference in either the electric or the magnetic properties of the two phases at the operating frequency. Water and hydrocarbons are examples of diamagnetic materials [37]. Water has a magnetic susceptibility ($\kappa'_m - 1$) of -9.05×10^{-6} [37]. Hydrocarbons with about 1 % of sulphur by weight have a static magnetic susceptibility in the range of $-5.2 \times 10^{-6} \rho_o$ to $-9.7 \times 10^{-6} \rho_o$ [38], where ρ_o is the density of hydrocarbons. The density of crude oil is approximately equal to 1. Hence, the difference between water and hydrocarbons in terms of magnetic properties is very slight. Therefore, it is not expected that magnetic fields would play a significant role in phase separation, and they will not be discussed any further.

On the other hand, the static relative permittivities of hydrocarbons and water are 2.13 and 81.1 [39], respectively. Therefore, the electric field is expected to have a significant influence on the physical behaviour of the emulsion. Such physical effects are discussed in section 3.6. The permittivity of a material, however, varies with frequency due to the relaxation/resonance mechanisms of polarization. Such a permittivity variation gives rise to dispersion regions and are discussed in section

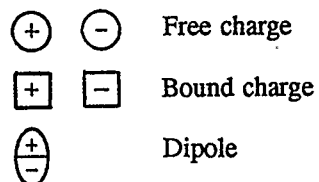
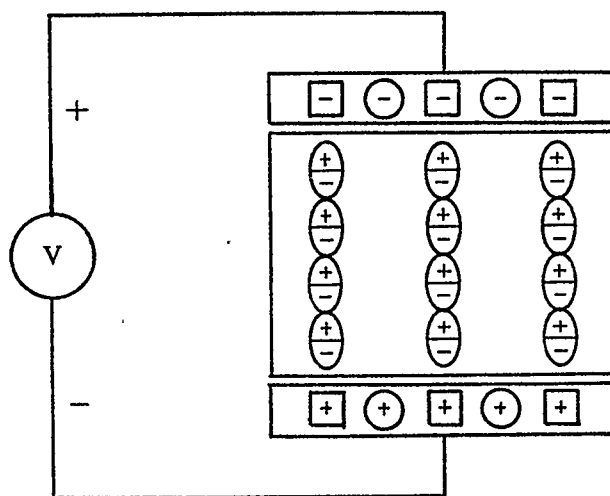
3.3. For a dispersed system, relaxation/resonance mechanisms may arise from polarization mechanisms that are due to the interfacial properties, as well as the bulk properties of the different phases [17, 34]. Various polarization mechanisms that are operative in a dispersed system are discussed in section 3.4.

3.3. Dielectric Polarization

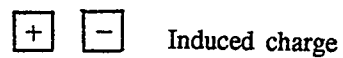
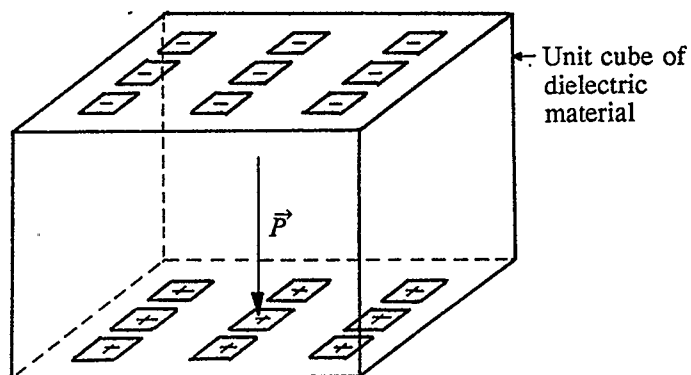
Dielectric polarization is the displacement of charges in a material forming dipole chains which align parallel to the field lines [40]. See Figure 3.2a. The complex permittivity is also a measure of dielectric polarization [41].

In order to express polarization in quantitative terms, a capacitor filled with a material and connected to a voltage source, as shown in Figure 3.2a, is considered. The end charges of the dipole chains are the induced charges on the material surfaces. These induced charges bind a fraction of the total (true) charges distributed over the surface area of the metal electrode, $q(1 - \frac{1}{\kappa^*})$ where q represents the total charges, and κ^* is the relative complex permittivity of the material. Note that only the free charges, $\frac{q}{\kappa^*}$, contribute to the voltage.

$$\begin{array}{ccccc}
 q & = & q(1 - \frac{1}{\kappa^*}) & + & \frac{q}{\kappa^*} \\
 \text{total} & & \text{bound} & & \text{free} \\
 \text{charges} & & \text{charges} & & \text{charges}
 \end{array} \tag{3.4}$$



a) Schematic representation of dielectric polarization



b) Schematic representation of polarization vector

Figure 3.2. Dielectric polarization [40].

The total charge density, the free charge density, and the bound charge density can be represented by vectors \vec{D} , \vec{E} , and \vec{P} , respectively, where \vec{D} is the *electric flux density*, \vec{E} is the *electric field intensity*, and \vec{P} is the *polarization vector*. These vectors are related in accordance with

$$\vec{P} = \vec{D} - \epsilon_0 \vec{E} \quad (3.5)$$

\vec{D} and \vec{P} are related to \vec{E} through

$$\vec{D} = \epsilon^* \vec{E} \quad (3.6)$$

and

$$\vec{P} = (\kappa^* - 1) \epsilon_0 \vec{E} \quad (3.7)$$

Equation (3.7) shows that the behaviour of a material in an electric field is governed by the polarization vector.

The polarization vector, \vec{P} , is similar to an electric dipole moment $\vec{\mu}_e$. An electric dipole moment $\vec{\mu}_e$ is produced by two identical charges q of opposite sign and a separation distance l . While the polarization \vec{P} is produced by the charge pairs induced on the surfaces of one unit cube of the dielectric material, as shown in Figure 3.2b. The polarization vector \vec{P} is therefore the electric dipole moment per unit volume of the material and can be expressed as

$$\vec{P} = N \vec{\mu}_e \quad (3.8)$$

where N is the number of electric dipoles per unit volume, and $\vec{\mu}_e$ is the average moment of the electric dipoles.

Dielectric polarization is a quality which varies with the electric field frequency. The frequency region where such an effect is observed is known as the *dispersion* region [41]. Dielectric dispersion is broadly classified into two types, resonance and relaxation.

Resonance dispersion [41] is associated with an atom or molecules making a transition from one energy level to another higher energy level as a result of interaction with the applied field. At the field frequency where this transition occurs, the *resonant frequency* (f_{res}), a characteristic sharp absorption peak is observable as shown in Figure 3.3. Examples of polarization mechanisms which give rise to resonance dispersion are electronic and atomic polarizations. Both of these polarization dispersions are observable only in the optical and infrared frequencies, respectively, and therefore do not concern us.

Relaxation dispersion [41] arises due to polarization mechanisms unable to keep in phase with the time varying field when the frequency is increased. The absorption peak of such a dispersion occurs at the *relaxation frequency*, $f_r = \frac{1}{2\pi\tau}$, where τ is the *relaxation time*. See Figure 3.4. Examples of polarization mechanisms which exhibit this type of dispersion characteristics are dipolar, normadic, interfacial, and counterion polarizations. The peak of the absorption characteristic (ϵ'' versus f), shown in Figure 3.4, represents the maximum electric field absorbed in the material.

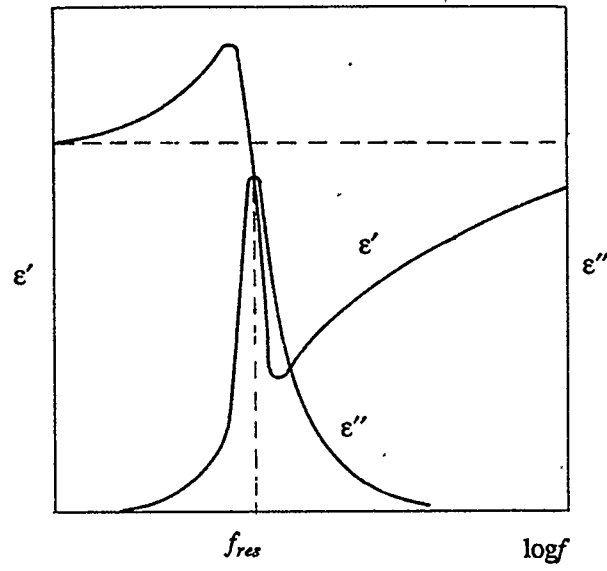


Figure 3.3. Resonance dispersion in dielectric media .

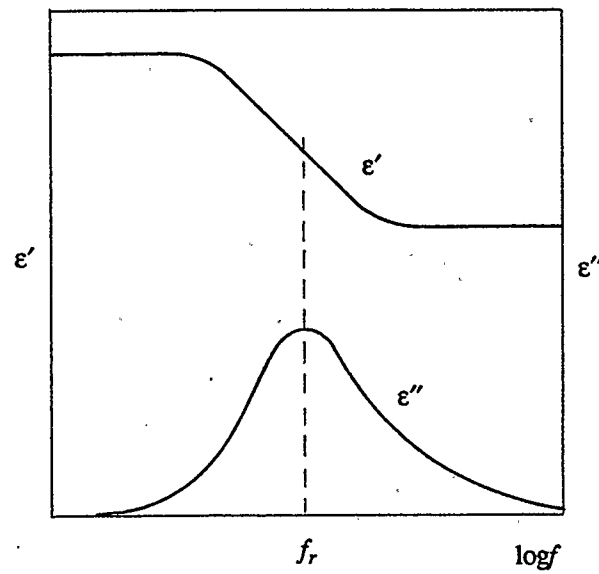


Figure 3.4. Relaxation dispersion in dielectric media .

3.4. Polarization Mechanisms

The polarization mechanisms which are operative in a dispersed system include normadic, electronic, atomic, dipolar (orientation), interfacial (Maxwell-Wayner type), and ionic double layer (counterion) polarizations. However, as mentioned earlier, electronic and atomic dispersions occur at optical and infrared frequencies, respectively, and therefore will not be observable in the present study. Normadic polarization, on the other hand, relaxes at approximately less than 10 kHz and again will not be observable in the present study.

There are two physical parameters which specify a relaxation polarization mechanism; the *characteristic relaxation time*, τ , and the magnitude of the *dielectric increment*, $\Delta\kappa$ [17]. $\tau = \frac{1}{2\pi f_r}$ specifies the frequency at which the mechanism is effective. $\Delta\kappa$ is the incremental change in the relative permittivity contributed by the individual polarization mechanism and hence is a measure of the intensity of that mechanism. Typical values for τ and $\Delta\kappa$ of the polarization mechanisms whose relaxation frequencies are between 10 MHz to 500 MHz are tabulated in Table 3.2, along with their characteristics. Dielectric dispersions of the various types of polarization mechanisms are also shown in Figure 3.5.

Dipolar (Orientation or Debye) Polarization

The asymmetric charge distribution of the unlike atoms of a molecule gives rise to a permanent dipole in the absence of an applied electric field [40, 17, 44]. If an

Type of polarization mechanisms	Bound counterion (Schwarz)	Diffuse counterion (Dukhin)	Interfacial (Maxwell-Wagner)	Orientation (Debye)
Typical f_r range (Hz)	100 k - 100 M [18]	100 - 100 k [18]	100 k - 100 M [18]	1 M - 100 G [18]
$\tau = \frac{1}{2\pi f_r}$ [17]	$\frac{a^2}{2\mu kT}$ [17]	$\frac{a^2}{2\mu kT}$ [17]	$\epsilon_o \frac{2\kappa_c + \kappa_d - \phi(\kappa_d - \kappa_c)}{2\sigma_c + \sigma_d - \phi(\sigma_d - \sigma_c)}$ [17]	$\tau \propto (\eta, \text{molecular diameter})$ [42]
Droplet size (dispersed phase) dependent of f_r	f_r increase with decrease in square of droplet radius [18,17]. See τ .	f_r increase with decrease in square of droplet radius [18,17]. See τ .	Independent	Independent [42]
Conductivity dependent of f_r			f_r increase with increase in σ_d or σ_c See τ .	f_r increase with increase in conductivity
ϕ dependent of f_r	Unknown	Unknown	Explicit dependence as shown in τ	Independent [40]
Temperature dependent of f_r	Thermally activated [42]	Thermally activated	f_r increase with increase in temperature	Thermally activated [42]
Typical $\Delta \kappa$	$1 - 10^3$ [18]	$1 - 10^6$ [18]	$1 - 10^5$ [18]	$1 - 160$ [18]
$\Delta \kappa$	$\frac{9}{4} \frac{\phi \epsilon^2 a \rho_s}{[1 + (\frac{\phi}{2})^2 \epsilon_o kT]}$ [17]	$\frac{9}{2} \rho_s \kappa_c [3 \frac{\epsilon^2 \kappa_c}{(kT)^2 6\pi\eta D_c} e^{\frac{\epsilon \kappa}{kT}} + e^{\frac{\epsilon W}{kT}}]^2$ [17]	$\frac{3\phi \kappa_c (\kappa_d - \kappa_c) [(\sigma_d + 2\sigma_c) - \phi(\sigma_d - \sigma_c)]^2 + 9\phi(1 - \phi)(\kappa_c \sigma_d - \kappa_d \sigma_c)^2}{[(\kappa_d + 2\kappa_c) - \phi(\kappa_d - \kappa_c)][(\sigma_d + 2\sigma_c) - \phi(\sigma_d - \sigma_c)]^2}$ [17]	

Table 3.2. Characteristics of various polarization mechanisms

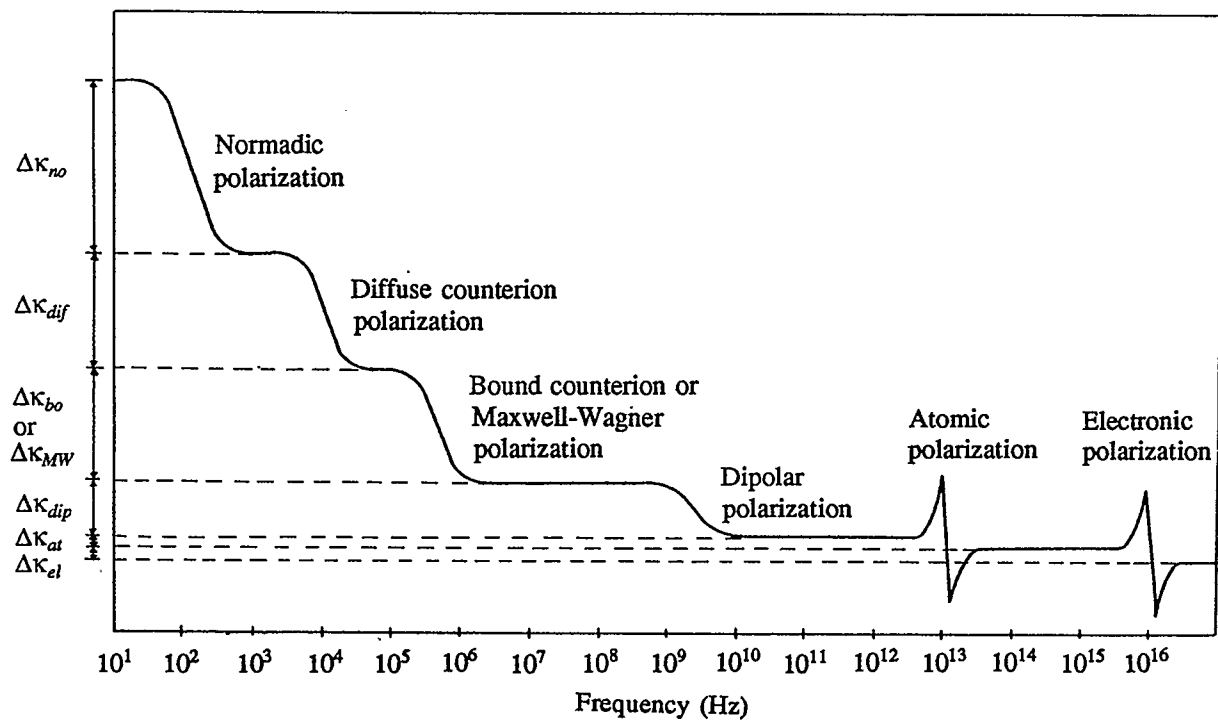


Figure 3.5. Dielectric dispersions of various polarization mechanisms [18].

electric field is applied, the dipoles experience a torque which causes them to align with the field direction. This results in *orientational* or *dipolar polarization*. The f_r for such a polarization mechanism is typically in the range of 1 MHz to 100 GHz, while the $\Delta\kappa$ is in the range of 1 to 160. f_r increases as the conductivity of the medium increases and as the temperature increases. Other characteristics of such a polarization are tabulated in Table 3.2.

Interfacial (Maxwell-Wayner) Polarization

In a dispersed system where different dielectric permittivities and conductivities exist in the two bulk phases, a disparity of charges will exist at the interface upon application of an electric field. Consequently, a highly effective polarization mechanism known as *interfacial* or *Maxwell-Wayner polarization* results [17]. The typical ranges of f_r and $\Delta\kappa$ are 100 kHz to 100 MHz and 1 to 10^5 , respectively[18]. f_r increases as the conductivity of either phase increases and as the temperature increases. The expression for τ is tabulated in Table 3.2.

Counterion Polarization

An anomalous polarization observed in liquid suspensions is another type of interfacial polarization. However, it does not arise because of the difference in the bulk properties between the two phases [17]. Schwarz attributes the anomalous polarization to the geometric redistribution of the *tightly bound counterions* at the outer Helmholtz plane (See [17] page 276). Dukhin attributes the anomalous polarization to the geometric redistribution of both the tightly bound and the diffuse

counterions [45]. According to Dukhin, there is an immediate distortion in the adjacent diffusion layer when the bound layer distorts due to the redistribution of the tightly bound counterions. In addition, he takes into consideration the possibility of the bound counterion exchange with the surrounding medium which is neglected by Schwarz. Dukhin, however, emphasizes that it is not so much the bound layer but the *diffuse layer* which contributes significantly to this polarization. The typical ranges of f_r and $\Delta\kappa$ for Schwarz type of counterion polarization are 100 kHz to 100 MHz and 1 to 10^3 , respectively; while the ranges for Dukhin type are 100 Hz to 100 kHz and 1 to 10^6 , respectively [17]. The characteristic frequencies for both types of counterion polarization increase as the square of the dispersed droplet radius decreases and as the temperature increases. Such a relationship can be seen in the expressions for τ shown in Table 3.2.

3.5. Dispersion in a Dispersed System

In a dispersed system, where the dielectric properties are different between the two phases, a dielectric dispersion may arise due to the relaxation effect in the bulk continuous phase or the bulk dispersed phase. In addition, the dispersion may occur due to the relaxation effect at the interface. The importance of a surface (interface) or bulk related relaxation effect in a dispersed system is dependent on the nature of the application. For instance, in phase separation of an emulsion, it is desirable to stress the emulsion at a electric field frequency where its aggregate stability is greatly reduced by the relaxation of those polarization mechanisms in the interface

and/or dispersed phase [32]. The above statement is clarified as follows. The applied electric field energy absorbed by the droplets, ϵ_d'' , is converted into kinetic energy. Such kinetic energy manifests itself in the form of physical behaviour, for instance, droplet coalescence and droplet collection. Hence, if an observed dispersion is due to the relaxation effect in the bulk dispersed phase, then the energy absorbed by the droplets is maximum at the characteristic frequency. In this case, the characteristic frequency corresponds to the optimum frequency of the involved physical behaviour.

Since the dispersed droplets are enclosed by protective envelopes, dispersions which arise due to relaxation effects in the protective interface (envelopes) may similarly play an important role in optimum droplet collection or droplet coalescence. Dispersions due to the relaxation effects in the bulk suspending phase, however, will have negligible effect on phase separation. This is because the electric field energy absorbed by the suspending phase is converted into kinetic energy in the molecules, giving rise to convectional effects.

A qualitative investigation of the dielectric properties of the system is therefore necessary to determine the different relaxation mechanisms operative in that system and their origin. From such an investigation, an attempt can then be made to explain the observed behaviour of the system under study.

3.6. Physical Effects on Dispersed Droplets

There are numerous physical effects observable in an emulsion under the influence of an electromagnetic field. These include orientation, mutual dielectrophoresis, "pearl chain" formation, droplet coalescence, and dielectrophoresis. The first four physical effects mentioned above are observable in both externally applied uniform and non-uniform electric fields. However, dielectrophoresis is only observable in an externally applied non-uniform electric field. Another physical effect known as electrophoresis, which will not be observable in the frequency range of the present investigation, will be discussed briefly together with dielectrophoresis.

3.6.1. Orientation

Orientation of suspended particles arises because of their non-spherical nature. A non-viable particle will normally orientate in such a way that its long axis is parallel to the field lines [19]. Consider a simple single electric dipole whose dipole moment makes angles with an external field, \vec{E} , as shown in Figure 3.6. As a result, torques are produced [37]. The torque about the negative charge has a magnitude $F_1 l \sin \theta_1$, while the torque about the positive charges has a magnitude $F_2 l \sin \theta_2$ (where $\vec{F}_1 = -q\vec{E}_{local}$, $\vec{F}_2 = +q\vec{E}_{local}$, and \vec{E}_{local} is the local electric field strength). The net resultant torque will tend to align the dipole with the field lines.

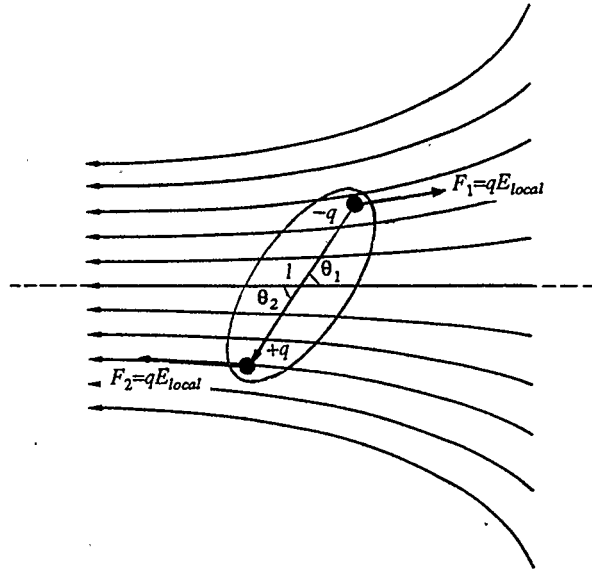
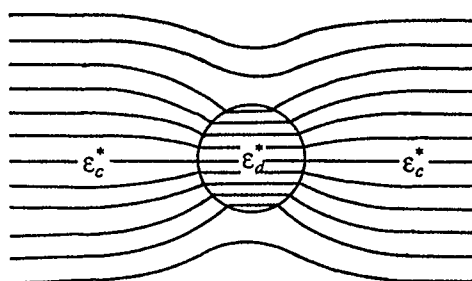


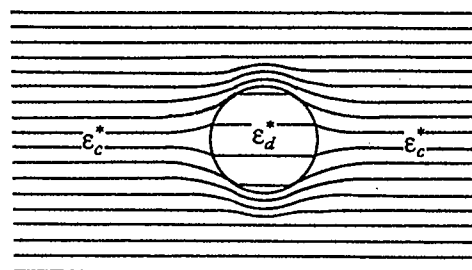
Figure 3.6. Orientation of an electric dipole.

3.6.2. Mutual Dielectrophoresis

In a dispersed system, a difference in the permittivity values of the dispersed and the continuous phase creates unequal field intensities in the two phases (see Figure 3.7). As a result, a local non-uniform electric field arises at the interface of the phases. When two or more neutral droplets are in close proximity, as shown in Figure 3.7b, their electric field gradient may create *mutual attraction* or *mutual repulsion* [17]. Depending on whether the *effective* absolute complex permittivity of the dispersed phase, $|\epsilon_d^*|$, is higher or lower than that of the continuous phase, $|\epsilon_c^*|$, mutual attraction or repulsion will result, respectively. Such a motion is known as *mutual dielectrophoresis* by Pohl [17].

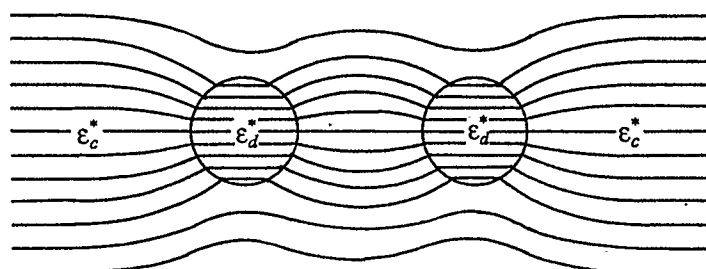


i) $|\epsilon_d^*| > |\epsilon_c^*|$

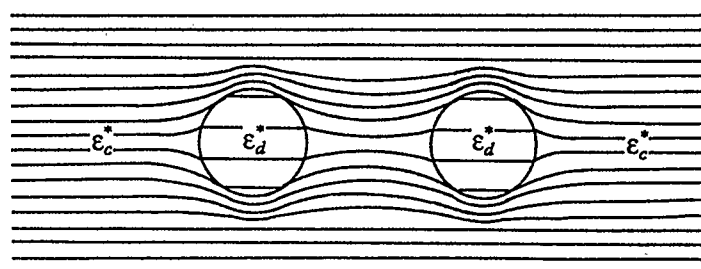


ii) $|\epsilon_d^*| < |\epsilon_c^*|$

a) Field distortion due to different permittivity values.



i) $|\epsilon_d^*| > |\epsilon_c^*|$; mutual attraction



ii) $|\epsilon_d^*| < |\epsilon_c^*|$; mutual repulsion

b) Resultant field distortion.

Figure 3.7. Mutual dielectrophoresis .

Notice that the term "effective" is used to take into account the permittivity values of the bulk dispersed phase, as well as that of the interface/surface.

3.6.3. "Pearl Chain" Formation

"*Pearl chain*" formation is a result of mutual attraction (see mutual dielectrophoresis, section 3.6.2) between the dispersed droplets and the alignment of these droplets along the field line. Hence, for "pearl chain" formation to occur the effective absolute complex permittivity of the dispersed phase must be higher than the suspending phase at the operating frequency.

Another condition for "pearl chain" formation is that the aligning force for the dispersed droplets must be greater than the randomizing force of Brownian motion. This condition requires the threshold field strength for "pearl chain" formation, $|E_{chain}|$, to be [24]

$$6S^2a^3\epsilon_c^*\phi |\vec{E}_{chain}|^2 = kT \quad (3.9)$$

where

$$S = \text{Re} \left\{ \frac{\epsilon_d^* - \epsilon_c^*}{2\epsilon_c^* + \epsilon_d^*} \right\}. \quad (3.10)$$

The threshold field strength is therefore frequency dependent through the frequency dependent nature of the complex permittivities of the two phases. In addition, it is lower for more concentrated emulsions, and larger dispersed droplet.

3.6.4. Droplet Coalescence

The process by which two droplets unite to become one is known as *droplet coalescence* [46]. Two droplets are capable of coalescing either due to collision or because they have remained in contact for a time long enough to allow *film drainage* (rupture of droplet envelopes in contact). In the absence of external force (at room temperature), droplet coalescence is possible because of Brownian motion which enhances droplet collision [34]. However, such motion decreases as the particle size increases, and is visible only in droplets of diameters less than 4 μm [31]. Nevertheless, droplet coalescence can be enhanced by an electric field due to head on collision of droplets as a results of mutual attraction, or a collision as a result of droplets travelling at different velocities in the same direction.

3.6.5. Dielectrophoresis (DEP)

Translation motion of a neutral dispersed droplet may be observed when the field is non-uniform. This is known as *dielectrophoresis (DEP)* [17]. Consider a neutral and a charged droplet in a uniform applied electric field as shown in Figure 3.8. The neutral droplet will merely be polarized while the charged droplet will be attracted to the oppositely charged electrode. In a non-uniform applied field, however, the neutral droplet will experience a translational force as shown in Figure 3.9. This occurs because the local fields, \vec{E}_{local} , operating at the two ends of the droplet are not equal, although the number of charges at each end are equal. As a

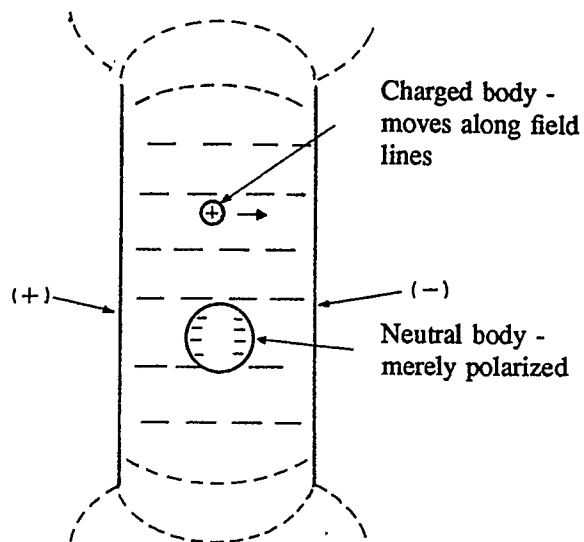


Figure 3.8. Uniform field (parallel plates electrode configuration).

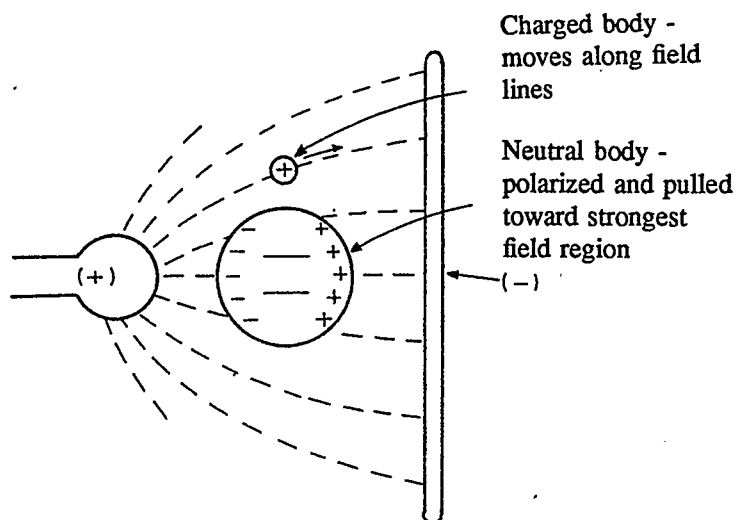


Figure 3.9. Non-uniform field (pin-plate electrode configuration).

result (since $\vec{F} = q\vec{E}_{local}$), the neutral droplet is pushed into or repelled from the higher field intensity regions, depending on whether the droplets are of a higher or lower permittivity than the continuous phase. The former and the latter motions are known as *positive DEP* and *negative DEP*, respectively. The charged droplet, on the other hand, will be attracted to the oppositely charged electrode. Such a motion is known as *electrophoresis* [17]. Since the charged droplets will merely vibrate about their original position according to the frequency of the ac field, at very high frequencies electrophoresis is no longer observable. This is because the net displacement is essentially zero. The DEP force, \vec{F}_D , exerted on the polarizable neutral droplet, however, is independent of the field direction. This could be seen also in the $\nabla |\vec{E}|^2$ term in equation 3.11 below [47].

$$\vec{F}_D = 2\pi a^3 K_e \nabla |\vec{E}|^2 \quad (3.11)$$

where

$$K_e = R_e \left\{ \epsilon_c' \frac{(\epsilon_d^* - \epsilon_c^*)}{(\epsilon_d^* + 2\epsilon_c^*)} \right\} \quad (3.12)$$

is the *effective excess permittivity* of the droplet in the continuous phase. The DEP force is dependent on the droplet size, the local field gradient, the electric field strength, as well as the effective excess permittivity of the droplet. DEP and mutual DEP differ in that the field non-uniformity in the former is externally applied, while in the latter it is the result of field distortion due to the presence of dispersed droplets having different permittivity values from the suspending medium. In a

non-uniform applied field if "pearl chain" formation is also favoured, then the formation of droplet chains and the movement of such chains towards the higher intensity field region (for the case $|\epsilon_d^*| > |\epsilon_c^*|$) will also be observable. The result of this in a wire-wire electrode configuration as shown in Figure 3.10 is the collection of droplet chains at the electrodes (the highest intensity field region). The number of droplets in a chain (i.e. the chain length) collected at the highest field intensity region, in a defined time, is known as *yield* or *dielectrophoretic collection rate*, DCR. The yields obtained over a range of frequencies give the yield spectrum.

DEP can be exploited in two ways. Firstly, it can be used as a means for separating materials of different dielectric properties. Secondly, the response of dispersed droplets (e.g. frequency dependent yield spectrum in batch DEP) to

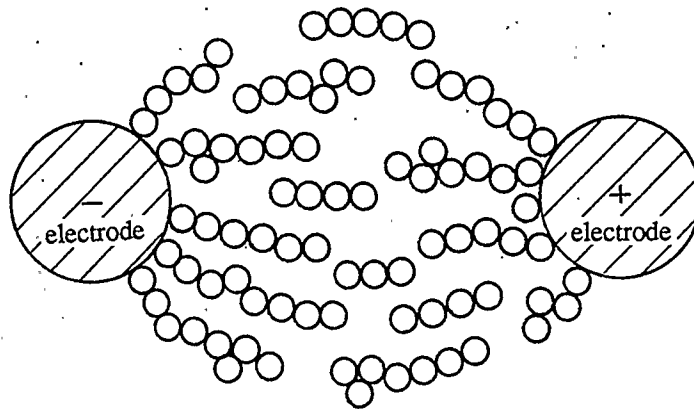
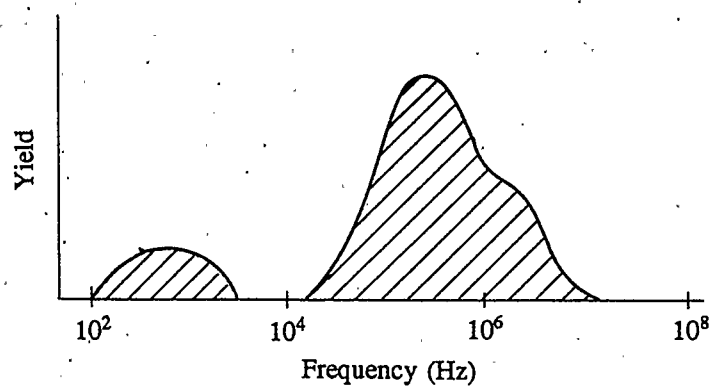


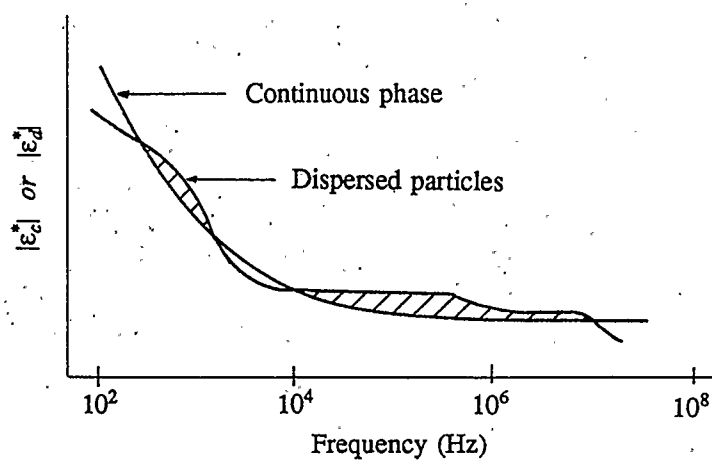
Figure 3.10. Collection of "pearl chains" at the electrodes [42].

dielectrophoresis can be measured to provide dielectric relaxation spectra [48]. As a separating technique for an emulsion, DEP collects the dispersed droplets into a specified region.

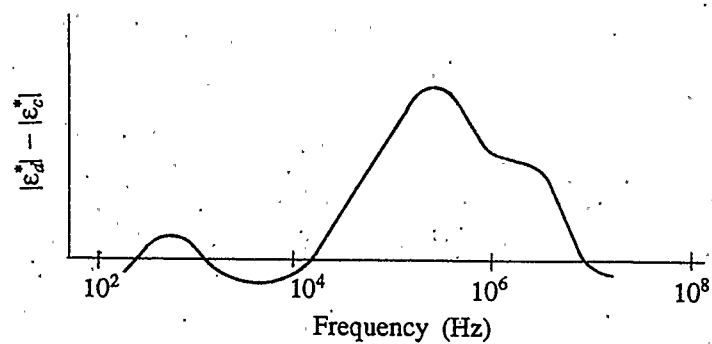
An interpretation of the yield spectrum for a system [17], obtained from DEP studies, is discussed as follows. Consider the obtained yield spectrum as shown in Figure 3.11a [17]. The collection rate of the dispersed particles exhibits three peak values. This implies that there are three different relaxation frequencies. There are also certain frequency ranges at which no droplet collection is observed. One possible explanation of such a dielectrophoretic response is that the effective polarizations of the dispersed particles and the suspending phase have characteristics as shown in Figure 3.11b. In the frequency ranges where particle collection (positive DEP) occurs, the effective absolute permittivity of the dispersed particles, $|\epsilon_d^*|$, is higher than that of the suspending phase, $|\epsilon_c^*|$. This can be seen by comparing the yield spectrum with the differential effective polarizations of the two phases shown in Figure 3.11c. Notice that the positive (shaded) regions in Figure 3.11b and Figure 3.11c correspond to the particle collection shown in Figure 3.11a. In the frequency ranges where there is no droplet collection at the region of highest field intensity, the effective absolute permittivity of the dispersed particles is lower than that of the suspending medium. The particles in this case are undergoing negative DEP.



a) Yield spectrum over a wide frequency range



b) $|\epsilon_c^*|$ and $|\epsilon_d^*|$ versus frequency



c) $|\epsilon_d^*| - |\epsilon_c^*|$ versus frequency

Figure 3.11. Interpretation of yield spectrum .

3.7. Techniques Used in the Present Studies

In this thesis, non-uniform electric fields are used to study the behaviour of the water-in-oil (w/o) emulsion over the frequency range of 10 MHz to 500 MHz. Non-uniform fields are chosen instead of uniform fields because all the physical effects, such as orientation, mutual dielectrophoresis, "pearl chain" formation, and droplet coalescence, which are observable in uniform fields are also observable in non-uniform fields. However, DEP is only observable in non-uniform fields. Since the peaks in the yield spectra obtained from dielectrophoresis studies are readily interpreted as dielectric relaxations, the application of non-uniform fields offers three advantages. Firstly, the physical behaviour of an emulsion under the influence of electric field can be determined. Secondly, it can be used as a separating technique in which all dispersed water droplets can be collected into an appropriate region. Thirdly, the dielectric dispersion in the emulsion system can also be determined.

The use of DEP in the determination of dielectric behaviour of an emulsion system offers various advantages as compared to conventional means. The conventional means of studying the dielectric properties of a material employ the bridge technique to measure the capacitance of an empty cell-condenser, as well as the capacitance and conductance of the cell-condenser filled with the material. Such a technique has the drawback that special care is required when applied to electrolyte solutions, especially at low frequencies [17]. This is because the ratio of the conductive component to the capacitive component is very large. The presence of streaming currents, due to the unevenness of the electrode surface, can also mask the

true conductive component of the system. Furthermore, stray capacitance can also produce a large and false polarization. Another disadvantage in the capacitance and conductance measurement is the requirement of a large emulsion sample.

In a w/o emulsion system, two water droplets are capable of coalescing either due to collision or because they have remained in contact for a time long enough to allow film drainage. Hence, the measured yield, obtained by counting the number of droplets in a chain after a defined time, is no longer a true representation of dielectrophoresis response. In addition, the concentration of the emulsion in each small sample varies. The DEP collection rate is known to be concentration dependent [18].

In view of the above problems, the average velocity of a single droplet is used in this thesis to reflect the dielectrophoresis response. Consider a water droplet in a non-uniform field as shown in Figure 3.12. Let \vec{F}_D be the dielectrophoretic force and \vec{F}_{drag} be the drag force. When the system is in equilibrium,

$$\vec{F}_D = \vec{F}_{drag} \quad (3.13)$$

For a spherical droplet, \vec{F}_{drag} is given as $6 \pi \eta \vec{v} a$, where η is the viscosity of the suspending phase, \vec{v} is the droplet velocity, and a is the droplet radius. Equation (3.13) becomes

$$2 \pi K_e a^3 \nabla |\vec{E}|^2 = 6 \pi \eta \vec{v} a \quad (3.14)$$

Therefore,

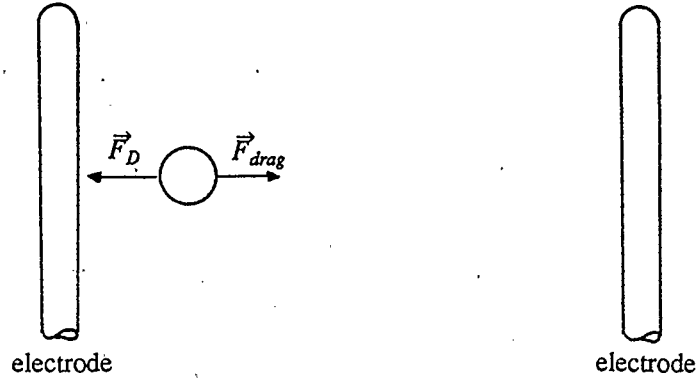


Figure 3.12. Forces on a droplet in a non-uniform field .

$$\begin{aligned} \vec{v} &= \frac{2 \pi K_e a^3 \nabla |\vec{E}|^2}{6 \pi \eta a} \\ &= \frac{1}{3} \frac{K_e}{\eta} a^2 \nabla |\vec{E}|^2 . \end{aligned} \quad (3.15)$$

Since η is a constant depending on the suspending phase, the droplet velocity is proportional to the dielectrophoretic force. Hence, a velocity spectrum will reflect the dielectrophoretic response.

In summary, non-uniform electric fields will be used to study the physical behaviour of the emulsion in the present work. This is because all physical effects observable in a uniform electric field are equally observable in a non-uniform electric field. In addition, droplet collection at the electrodes which is an end result of dielectrophoresis and only occurs in non-uniform fields can also be observed. The

optimum frequencies for droplet collection will be determined from the velocity spectra of various droplet sizes, obtained from dielectrophoresis studies, over the frequency range of 10 MHz to 500 MHz.

CHAPTER 4

EXPERIMENTAL

4.1. Experimental Requirements

One of the requirements of the experimental setup is the production of a non-uniform electric field within the emulsion sample, so that dielectrophoresis is observable. Secondly, the chamber which holds the emulsion must allow monitoring of the emulsion with the aid of an optical microscope. To meet these requirements, a special chamber was constructed from a printed circuit board. A hole, 10 mm in diameter, was drilled through the printed circuit board to enable observations using the microscope. A wire-wire electrode configuration, as shown in Figure 4.1a was housed within the hole to generate the required non-uniform field. Such a configuration was chosen because it is simple and easy to construct compared to the other configurations shown in Figure 4.1. The chamber is discussed in greater detail in section 4.2.1.

The experimental setup should also be capable of monitoring the voltage applied across the emulsion sample. The theoretical setup used to study the behaviour of the emulsion is shown in Figure 4.2. The load in Figure 4.2 consists of the emulsion sample under investigation together with the chamber which holds the sample. The return loss for the emulsion sample together with the chamber was measured using a network analyser (HP 8085A), and is shown in Figure 4.3. *Return*

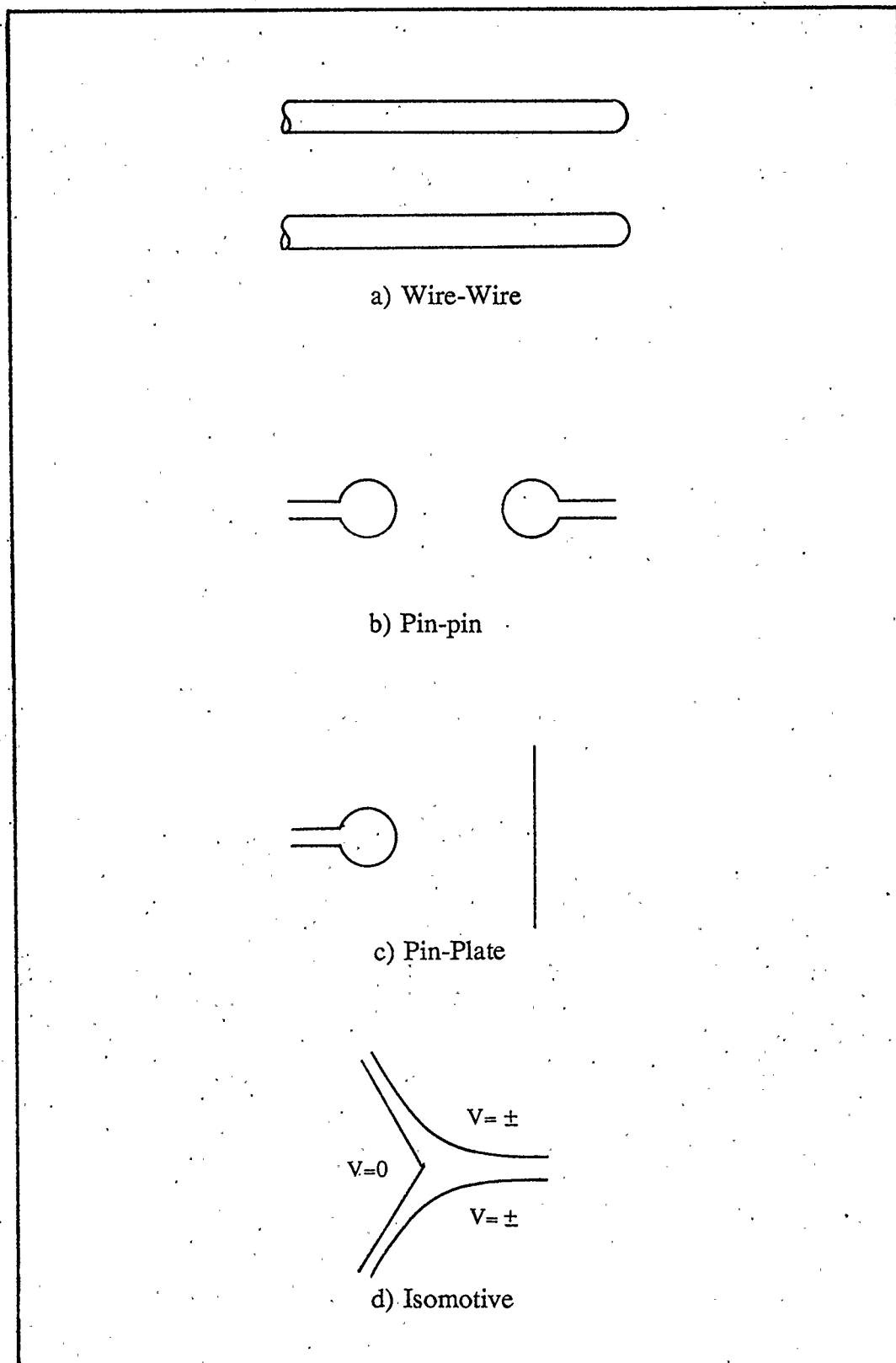


Figure 4.1. Various electrode shapes for producing dielectrophoretic fields [18].

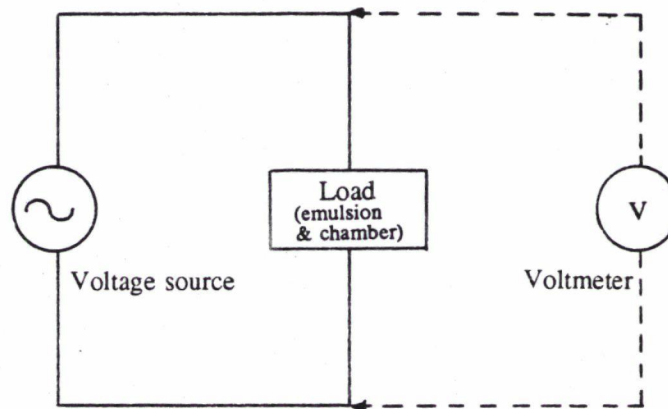


Figure 4.2. Theoretical setup .

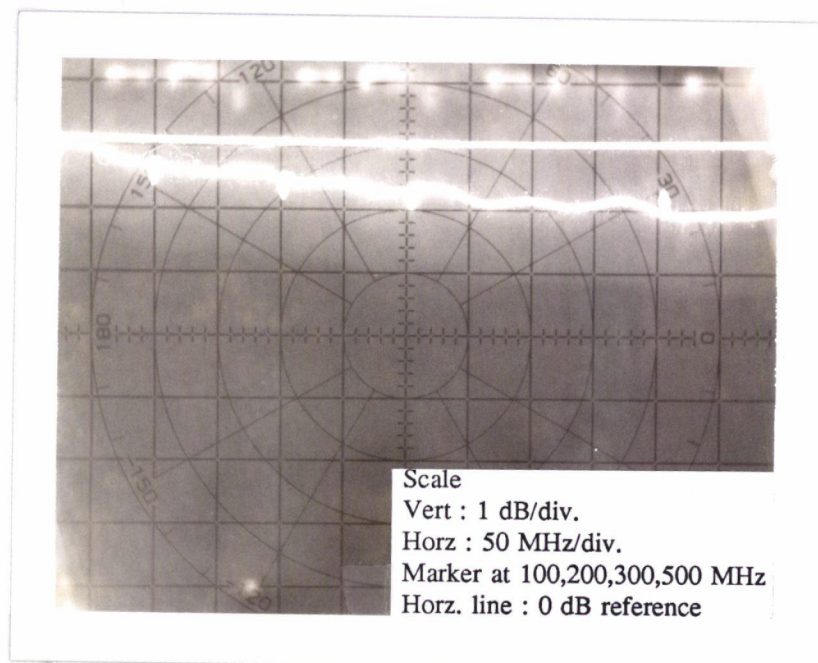


Figure 4.3. Return loss of the load .

loss is defined as the ratio of the reflected voltage to the incident voltage in decibels (dB). Figure 4.3 shows that a standing wave exists within the frequency range studied. This means that the impedance of the load is not matched to that of the source. Hence, the reading on the voltmeter in Figure 4.2 is essentially a measurement of the standing wave voltage which is a function of the electrical length. (An electrical length is a length expressed in terms of wavelength). In other words, the reading on the voltmeter depends on the position at which the voltmeter is inserted. In addition, the electrical length varies with frequency. In order to determine the voltage applied to the load, irrespective of the frequency of applied voltage, a directional coupler together with a vector voltmeter was employed. In this case, the voltage at the load is equal to the summation of the incident and the reflected voltages.

4.2. Experimental Setup and Apparatus

A block diagram of the experimental setup is shown in Figure 4.4. The signal source used in this study consisted of a signal generator (Marconic Instrument 2022). The output from this source is amplified using a power amplifier (Boonton Radio Company type 230A) to provide a voltage of 10 Vrms across the electrodes. The signal is coupled to the load through a directional coupler. The directional coupler allows the incident and the reflected waves at the load to be directed to a vector voltmeter (HP 8045A). The vector voltmeter measures both the incident and the reflected voltages. A 10 dB attenuator is inserted at the input to each probe of the

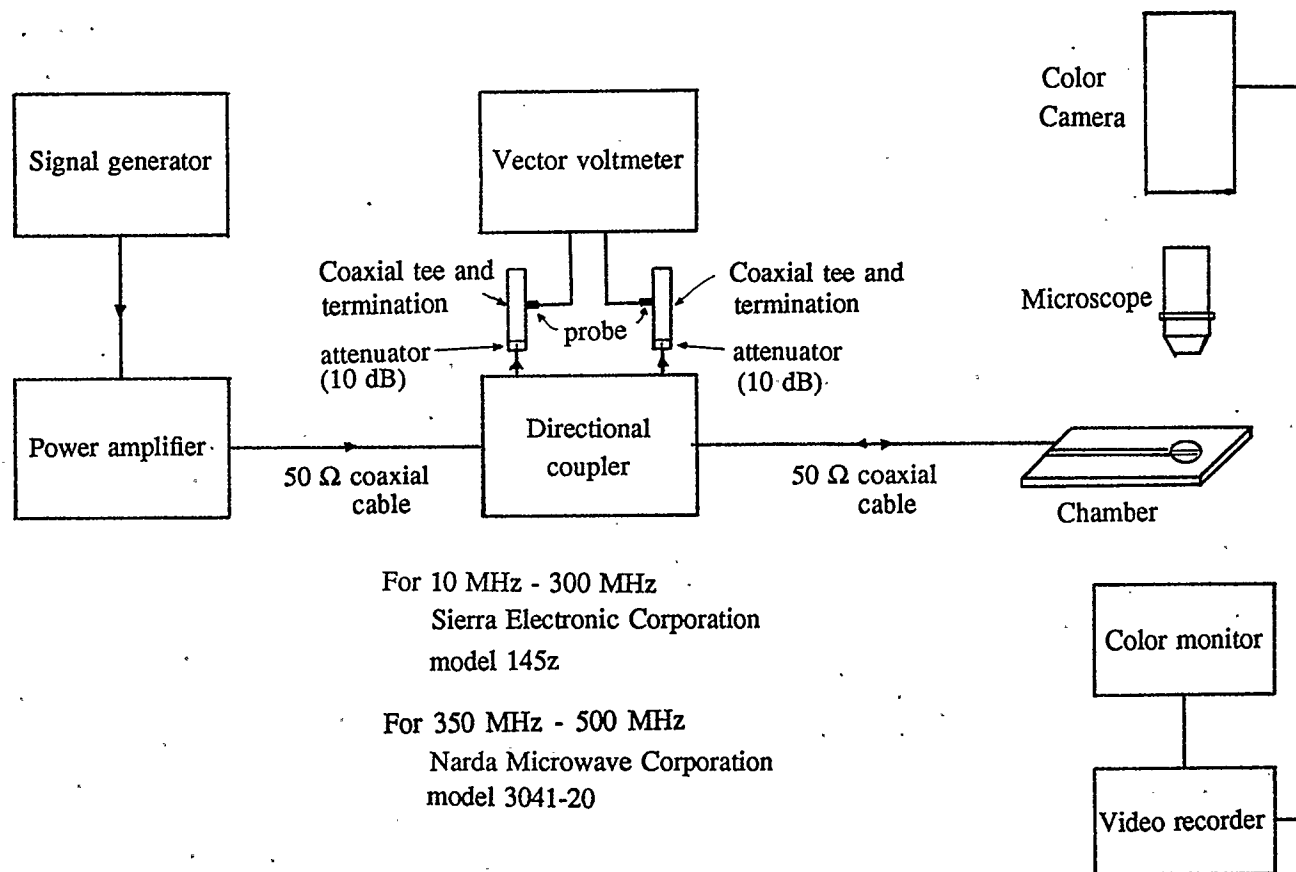
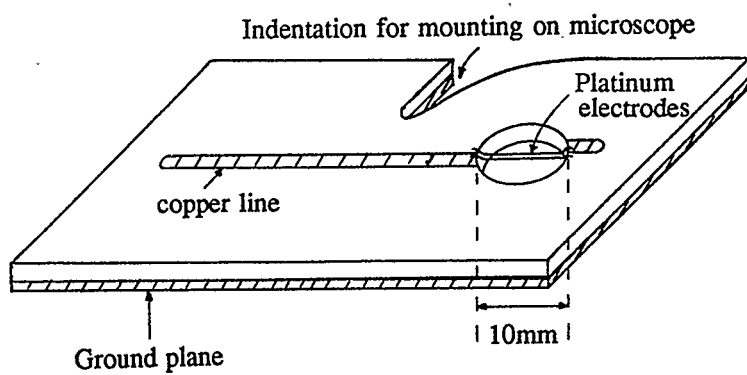


Figure 4.4. Experimental setup for studying field effects on w/o emulsion .

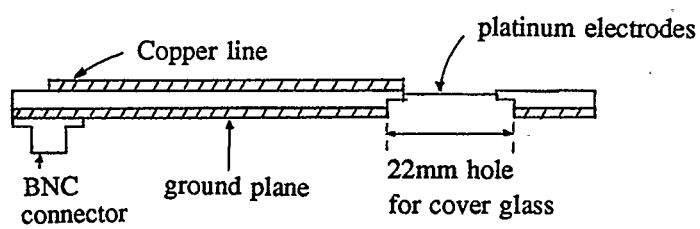
vector voltmeter to prevent damage to the vector voltmeter probes. The behaviour of the emulsion under the influence of the electromagnetic field was observed with the aid of an inverted optical microscope (Leitz Diavert) fitted with X32 objective and X10 ocular. A color television camera (Panasonic WV-CD01) is fitted onto the microscope to allow the emulsion sample to be displayed on a color monitor (Panasonic CT-9072MC), and simultaneously recorded using a video recorder (Sony VO-2600). In the second part of the experiment, where time measurement is required to compute the droplet velocity, a mechanical timer (Jaquet) is used.

4.2.1. The Chamber

The chamber used in this investigation is shown in Figure 4.5. It is constructed from a printed-circuit board with a 10 mm diameter hole on one end to allow observation with the microscope and to facilitate cleaning of the chamber. On the back side of the board is the ground plane and another hole. This hole, slightly greater than 22 mm in diameter, is concentric to the observation hole and bored to a depth of 0.25 mm. It is used to secure a 22 mm cover glass which holds the sample. Two parallel platinum wire electrodes (diameter = 0.13 mm), 0.165 mm apart, are placed in the centre of the chamber housing to produce an *approximately* cylindrical non-uniform field near the vicinity of each platinum wire. One of the electrodes is connected to the ground plane, while the other is connected to the 2.375 mm-wide copper line on the top side of the chamber. The copper line together with the ground plane and the fibre glass board, essentially form a 50 Ω microstrip line



a) 45 degree view



b) Cross-sectional view

Figure 4.5. The Chamber .

which matches the 50 Ω coaxial cable. The indentation on one edge of the chamber aids in mounting the chamber securely onto the microscope stage.

4.2.2. The Directional Couplers Used

For frequencies in the range of 10 MHz to 300 MHz, a Siera Electronic Corporation (SEC) 145z directional coupler was used. The variation of the coupling factor with frequency is shown in Figure 4.6. For frequencies in the range of 350 MHz to 500 MHz, on the other hand, a Narda Microwave Corporation (NMC) 3041-20 directional coupler was used. This is a -20 dB coupler with a lower cutoff frequency of 500 MHz. It was calibrated with a 50 Ω load at 350 MHz, 400 MHz, and 450 MHz for use at these frequencies. The coupling factors for these frequencies are shown in Table 4.1.

The following example calculates the required voltage reading on the vector voltmeter, in order to ensure that 10 V_{rms} is applied across the electrodes. Let V_L be the load voltage which is the voltage across the two electrodes. In which case, $V_L = 10 V_{rms}$. Since impedance matching between the source and the load is not achieved, the load voltage is the summation of the incident voltage, V_I , and the reflected voltage, V_R , as shown in Figure 4.7. Hence,

$$V_L = V_I + V_R = 10V_{rms} \quad (4.1)$$

At 300 MHz, from Figure 4.7, the coupling factor of the directional coupler is -12 dB. The attenuator in front of each individual probe of the vector voltmeter

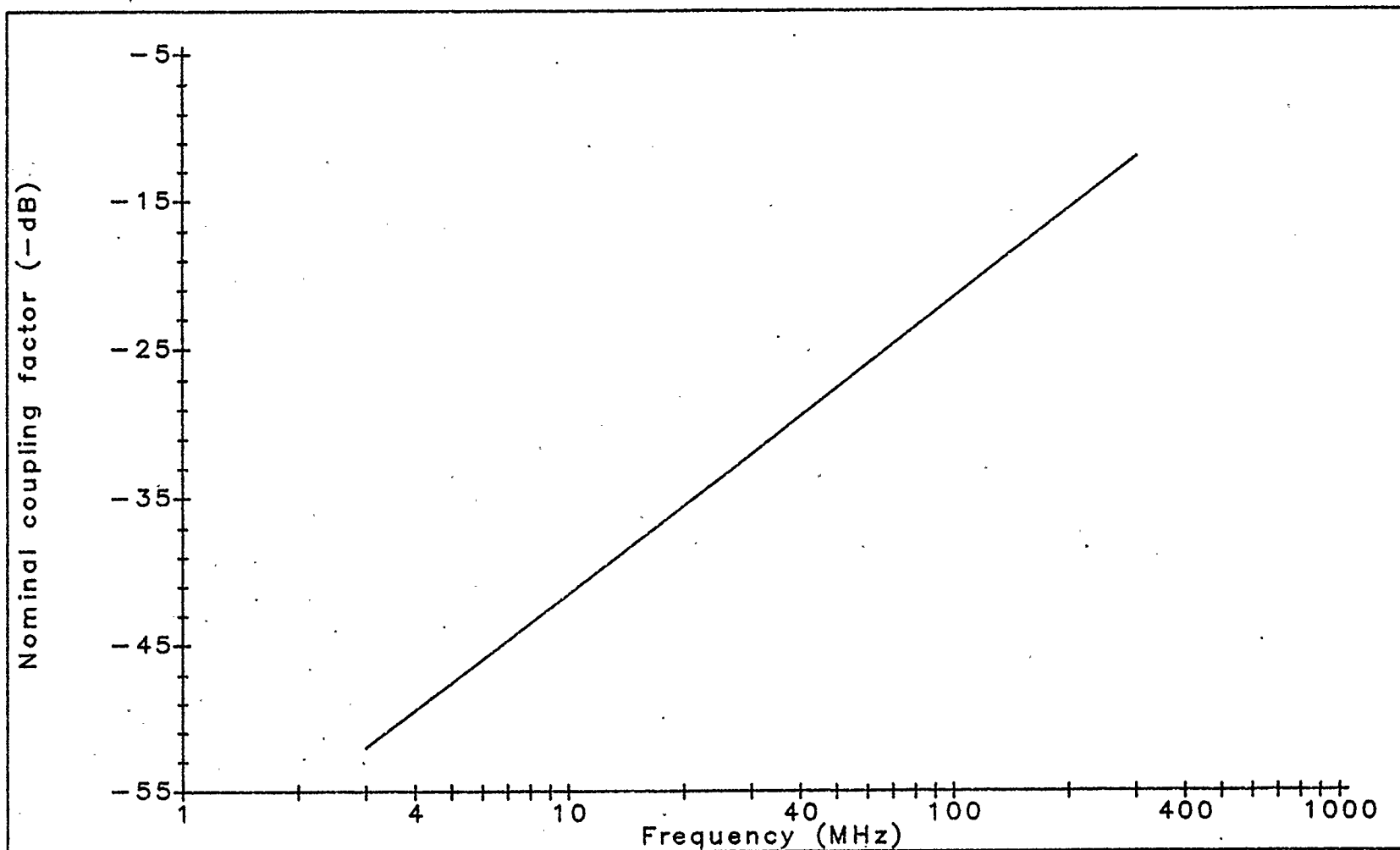


Figure 4.6. Coupling factor of SEC-145z directional coupler .

Frequency	Coupling Factor
350 MHz	-20.5 dB
400 MHz	-20.3 dB
450 MHz	-19.8 dB

Table 4.1. Coupling factor of NMC-3041-20 directional coupler .

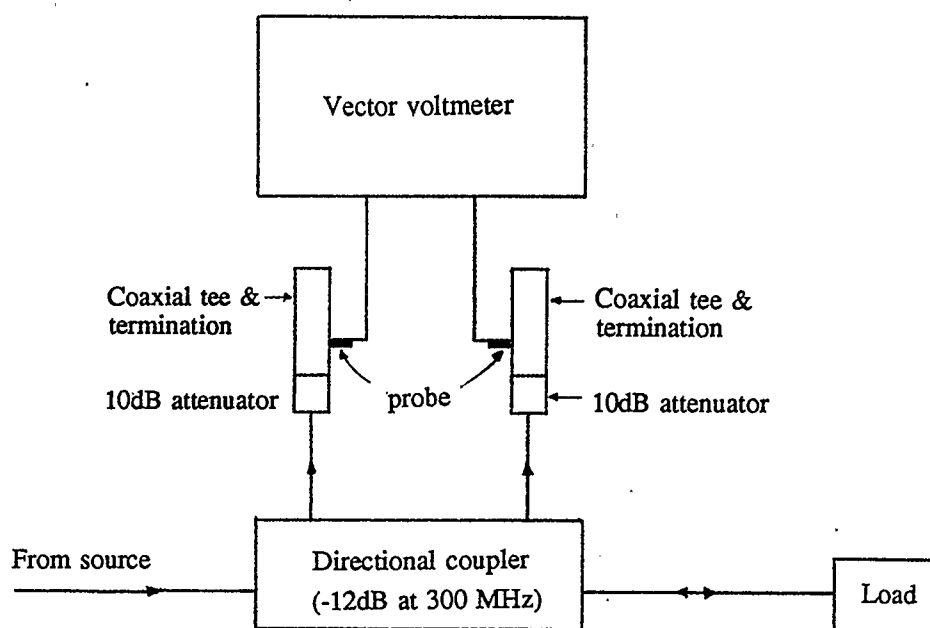


Figure 4.7. Voltage at the load .

contributes an additional -10 dB. The total attenuation is therefore -22 dB. Let the sampled incident voltage and the sampled reflected voltage be V_{IS} and V_{RS} , respectively. The relationship between the sampled load voltage, $V_{IS} + V_{RS}$, and the actual load voltage, $V_I + V_R$, is given by

$$-22\text{dB} = 20 \log \frac{V_{IS} + V_{RS}}{V_I + V_R} \quad (4.2)$$

Therefore, to ensure that 10 Vrms is applied at the two electrodes, $V_{IS} + V_{RS}$, which is the summation of the vector voltmeter readings for the sampled incident and sampled reflected voltages, must be equal to 794.3 mVrms.

4.2.3. The W/O Emulsion Used

The water-in-oil (w/o) emulsion used in this study was provided by Geotech Engineering (Calgary). The emulsion contained 0.529 and 0.001 volume fractions of water and sediment, respectively. The sizes of the water droplets ranged from 1.1 μm to 7.9 μm . The conductivity of the emulsion was 89.2×10^{-6} mho/m at 1 kHz when measured with the conductivity cell (YSI 3403).

4.3. Experimental Procedures

The experimental work consisted of two parts. In the first part the physical behaviour of the emulsion under the influence of the electromagnetic field was studied. This behaviour included orientation of aggregate droplets, mutual attraction,

"pearl chain" formation, droplet coalescence, and droplet collection. In the second part the optimum frequency (or possibly range of frequencies) for droplet collection at the electrodes was determined. All the experiments were carried out at room temperature.

4.3.1. Part 1 : Physical Behaviour of the Emulsion

A circular cover glass was secured to the bottom of the observation chamber, using a small quantity of silicone grease. A fixed volume of w/o emulsion was drawn with a syringe and placed into the observation chamber using a technique developed by Robertson *et. al.* [49]. The emulsion was essentially sandwiched between two layers of voltesso (an oil) to avoid contact with the glass surface. This prevented the water droplets in the emulsion from sticking onto the hydrophilic glass surfaces. At the same time it enabled the opaque nature of the emulsion to be viewed under a microscope. The chamber was mounted onto the microscope. A voltage of 10 Vrms was applied across the two electrodes and the behaviour of the emulsion was monitored. This was accomplished with the aid of a microscope and recorded on a video tape over the frequency range of 10 to 500 MHz.

4.3.2. Part 2 : Optimum Frequency for Droplet Collection

In this part of the experiment, the time taken for a droplet of diameter $5.1\text{ }\mu\text{m}$ to travel a known distance was measured. This known distance was $25.4\text{ }\mu\text{m}$ away

from either electrode surface as shown in Figure 4.8 (1 division of the graduated reticle in the microscope eyepiece corresponds to $25.4\text{ }\mu\text{m}$). In a manner similar to the previous description in section 4.3.1, the sample was placed into the chamber and the chamber was mounted onto the microscope stage. The droplet size was measured with a circular template placed on the face of the television monitor. It was then calibrated with a known size of polystyrene microspheres (Duke Scientific). The position of the droplet was monitored with the aid of a graduated reticle in the eyepiece of the microscope. In most cases, the droplet was moved with the help of the field to the starting position ($25.4\text{ }\mu\text{m}$ away from either electrode; see Figure 4.8). The field was then removed to ensure that the droplet monitored was initially at rest. The timer was started when the field was reapplied to move the droplet from starting position, and stopped when the droplet came into contact with the electrode. The *average* droplet velocity was computed by dividing the travelled distance ($25.4\text{ }\mu\text{m}$) over the time measured. By varying the the applied field frequency, a spectrum of droplet velocities was obtained for $5.1\text{ }\mu\text{m}$ droplets in the frequency range of 10 MHz to 500 MHz. Another spectrum was obtained for $4.25\text{ }\mu\text{m}$ droplets for the same emulsion.

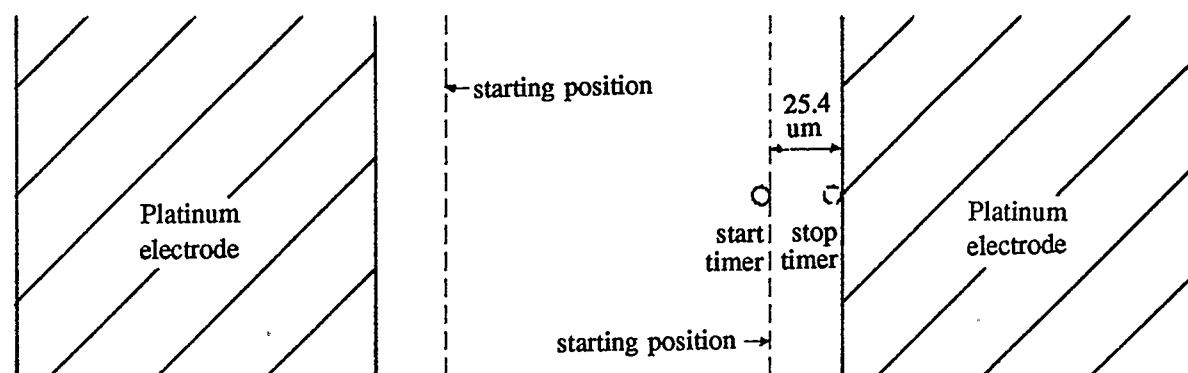


Figure 4.8. The distance travelled by the droplet.

CHAPTER 5

RESULTS AND DISCUSSION

5.1. Part 1 : Physical Behaviour of the Emulsion

Figure 5.1a shows the water droplets dispersed in the oil of the water-in-oil (w/o) emulsion sample under study. The water droplets were observed to be dispersed as discrete spheres, as well as in aggregate forms. Figure 5.1 shows the w/o emulsion before and after being exposed to a non-uniform ac electric field. Although Figure 5.1 was obtained at 450 MHz, it is representative of the emulsion behaviour throughout the frequency range of 10 MHz to 500 MHz. Various physical effects were observed in the emulsion upon application of the electric field. Figures 5.2 and 5.3 are magnified sections of Figure 5.1. Figure 5.2 shows the orientation of an agglomerate water droplet with the long axis parallel to the electric field lines. Figure 5.3 shows mutual attraction between neighbouring droplets. Such a behaviour indicates that $|\epsilon_d^*| > |\epsilon_c^*|$ in the frequency range of 10 MHz to 500 MHz, as discussed in section 3.6.2. Sometimes, mutual attractions were followed immediately by the orientation of the droplets along the field lines, as shown in Figure 5.4. This occurs because the mutually attracted droplets possess a long axis which makes an angle with the electric field lines. Spontaneous droplet coalescence was also observed when droplets experienced mutual attraction. This is shown in Figure 5.5. However in this study, "pearl chain" formation along the electric field lines was the

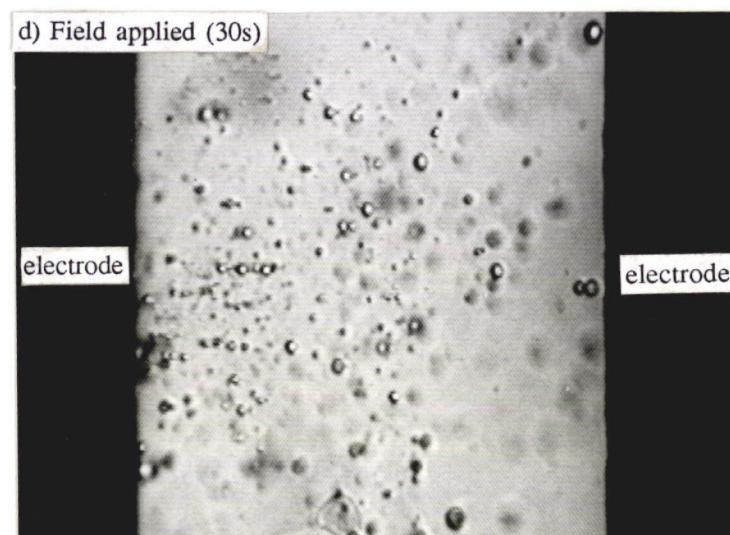
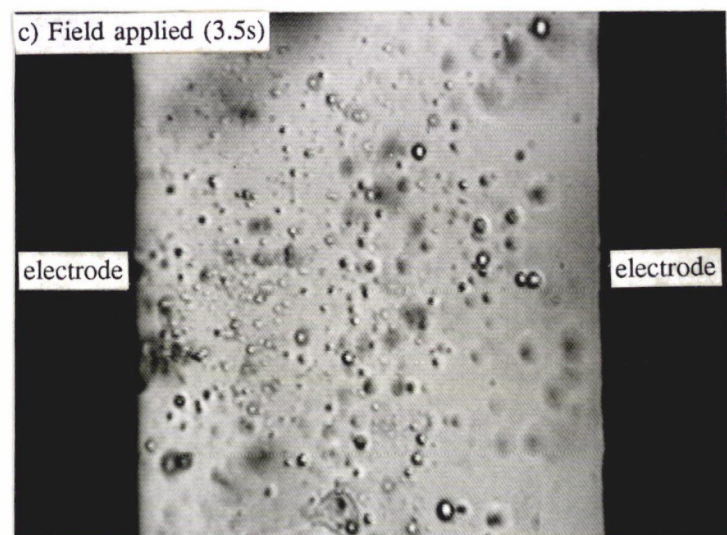
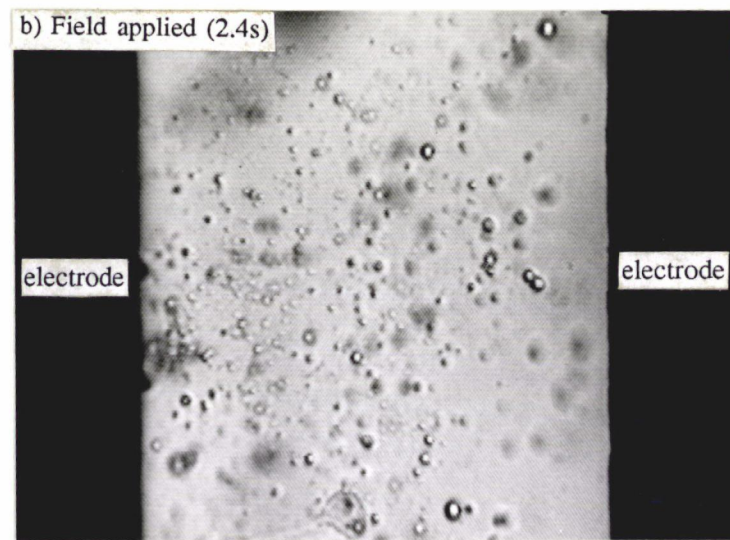
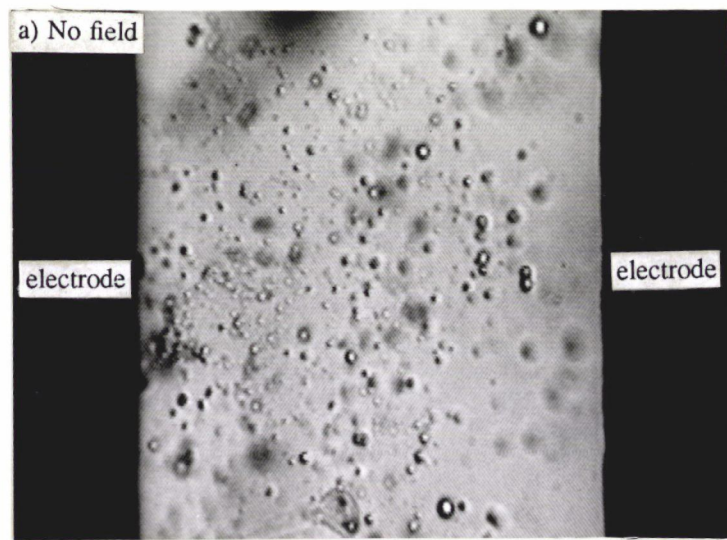


Figure 5.1. Effect of electric field on w/o emulsion.

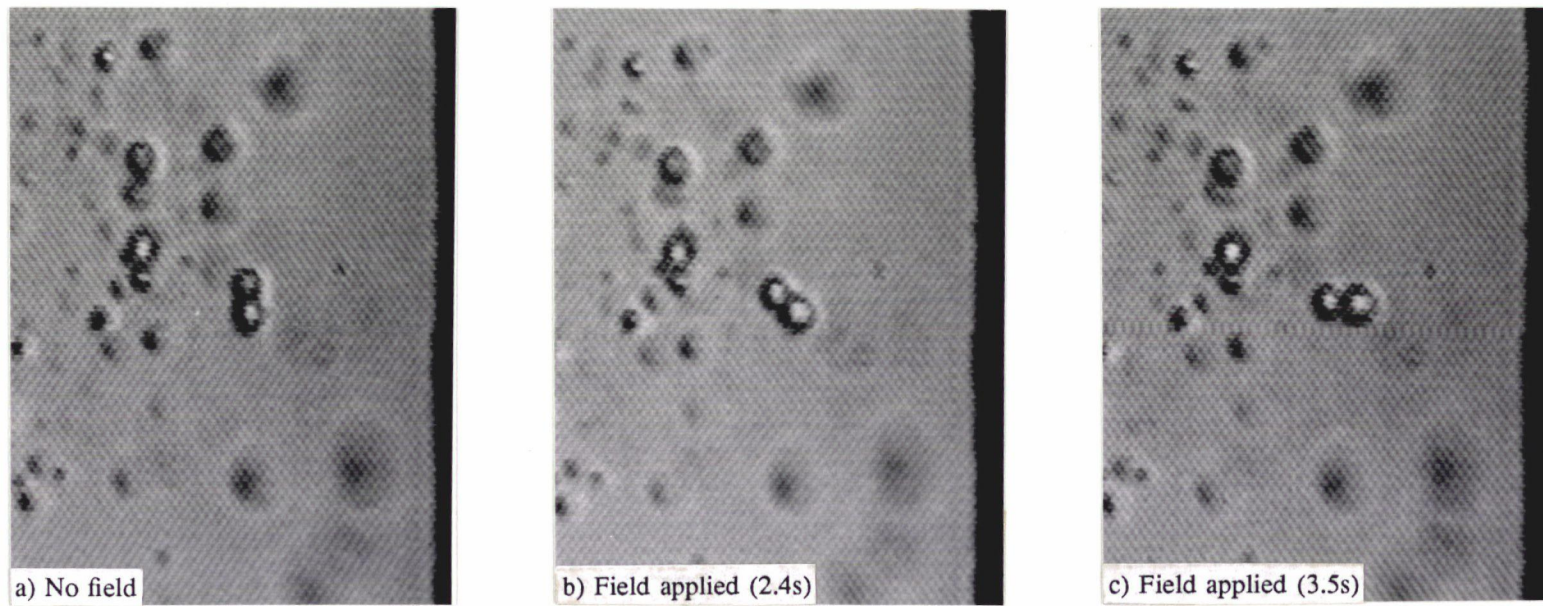


Figure 5.2. Orientation of agglomerate droplets.

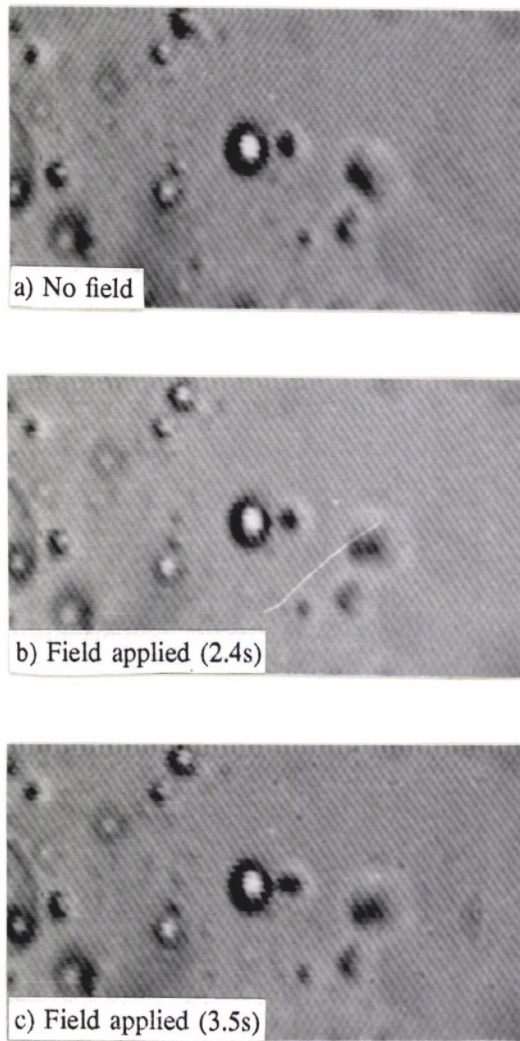


Figure 5.3. Mutual attraction between droplets.

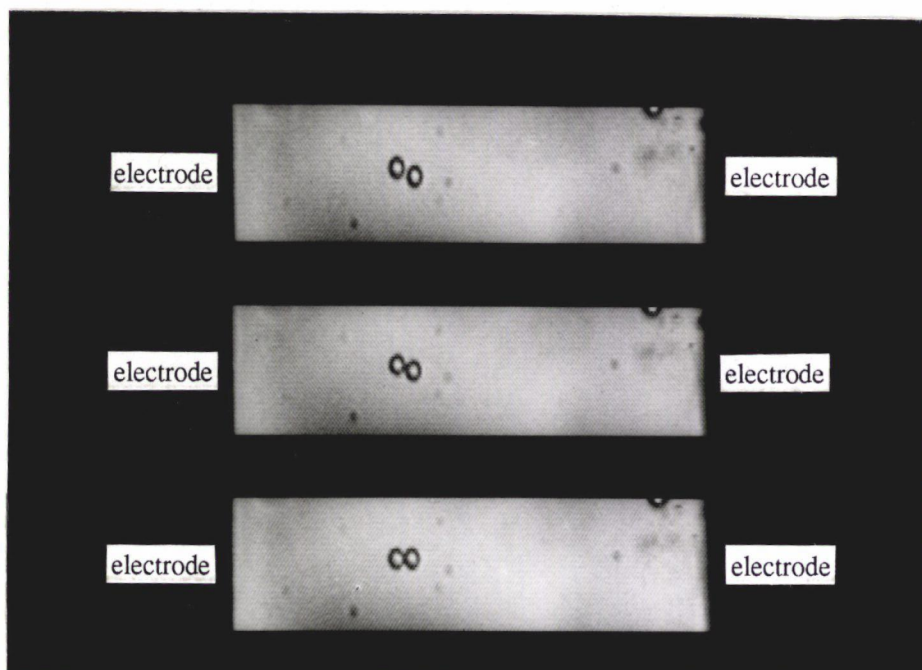


Figure 5.4. Orientation of mutually attracted droplets.

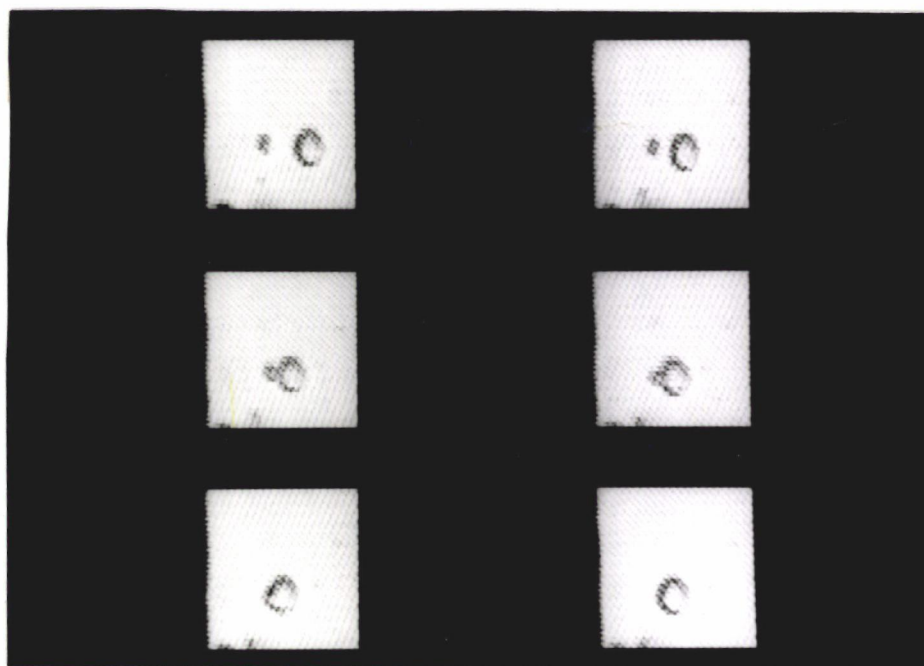


Figure 5.5. Spontaneous droplet coalescence.

more dominant result of mutual attraction, compared to droplet coalescence. This can be seen in Figure 5.6. Some droplets were also observed to remain in discrete form upon the application of the electric field. This is because they are not in close proximity to other droplets. For example, when both droplets are approximately $5.38 \mu\text{m}$ in diameter, a distance between droplet centres of at least $8.03 \mu\text{m}$ is required for the droplets to remain in discrete form. The most noticeable effect observed after the application of field was the translational motion of droplets (aggregate form, discrete form, and "pearl chain") towards the electrode surfaces. Such a behaviour is to be expected as all droplets experienced an increasing electric field intensity as they moved nearer to the electrodes. For the same reason, the velocities of the droplets were observed to increase as the droplets moved closer to the electrodes. Such behaviour is in accordance with the dielectrophoretic force, given by equation (3.11) as $\vec{F}_D = 2 \pi a^3 K_e \nabla |\vec{E}|^2$, which indicates that as $\nabla |\vec{E}|^2$ increases, $|\vec{F}_D|$ also increases. Figure 5.7 shows the electric field distribution for a parallel wire-wire electrode configuration (in cross-section). Note that $\nabla |\vec{E}|$ increases as the distance from either electrode decreases. Hence, as droplets approach the electrodes, $|\vec{F}_D|$ increases causing the acceleration of droplets. As discrete droplets, aggregate droplets, and droplet chains moved toward the electrodes, collision, as well as further mutual attraction, chain formation, and coalescence were observed. After about one minute, the collection of water droplets at the electrodes, in the form of chains, became visually noticeable as can be seen in Figure 5.8.

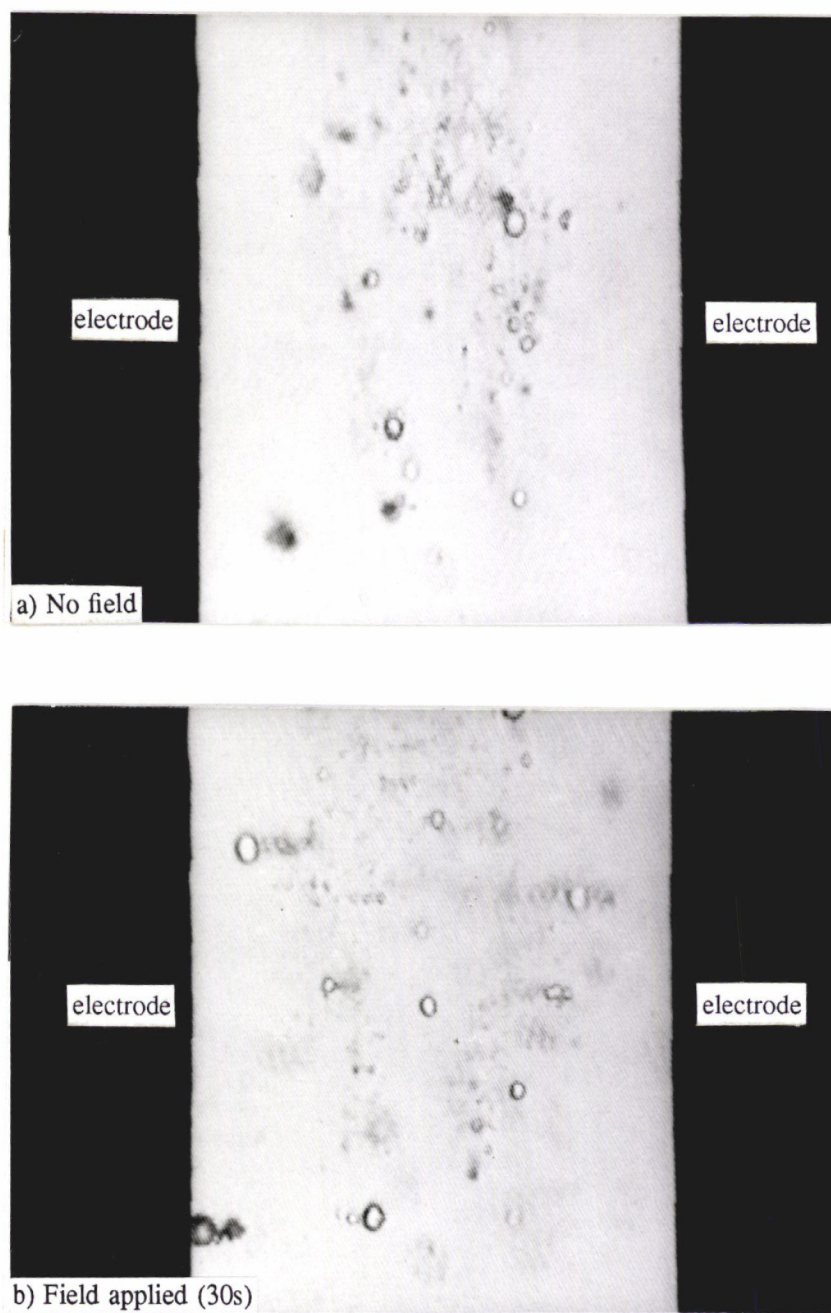


Figure 5.6. "Pearl chain" formation.

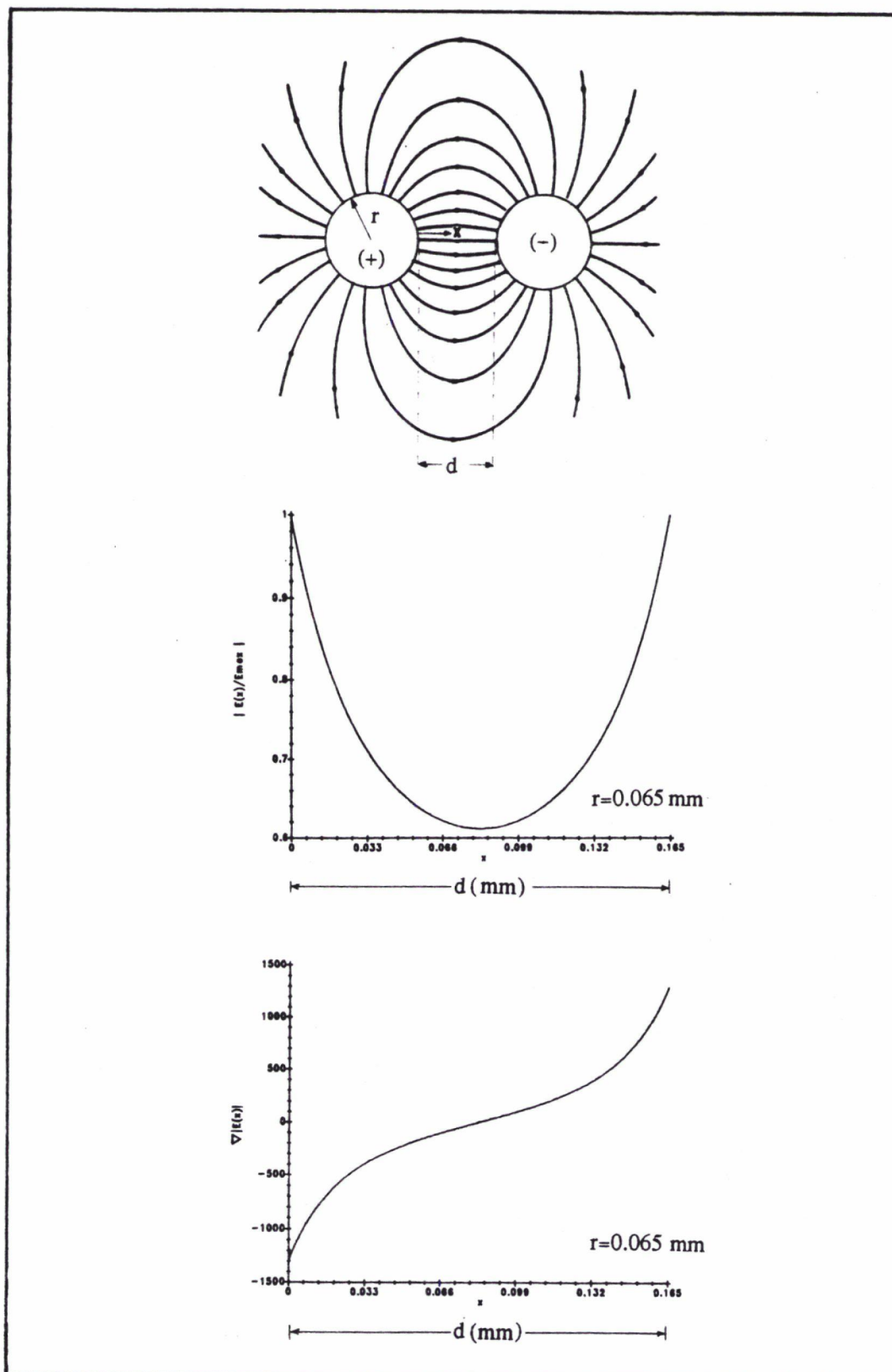


Figure 5.7. Electric field distribution in a wire-wire electrode configuration [50].

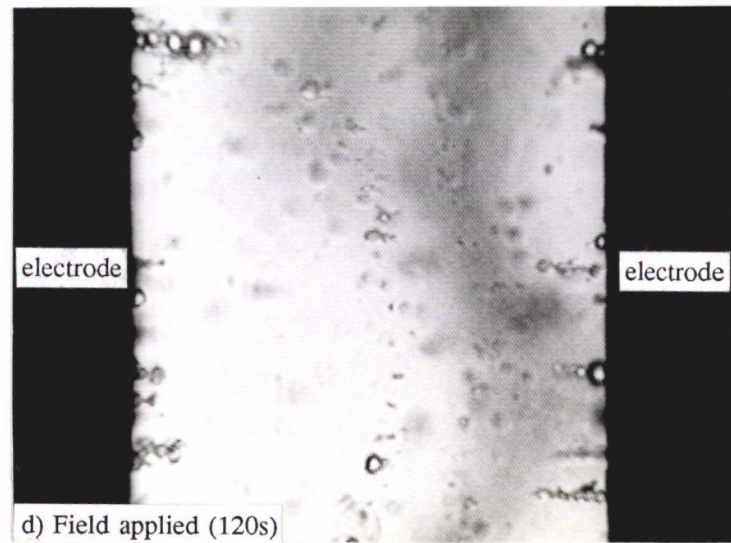
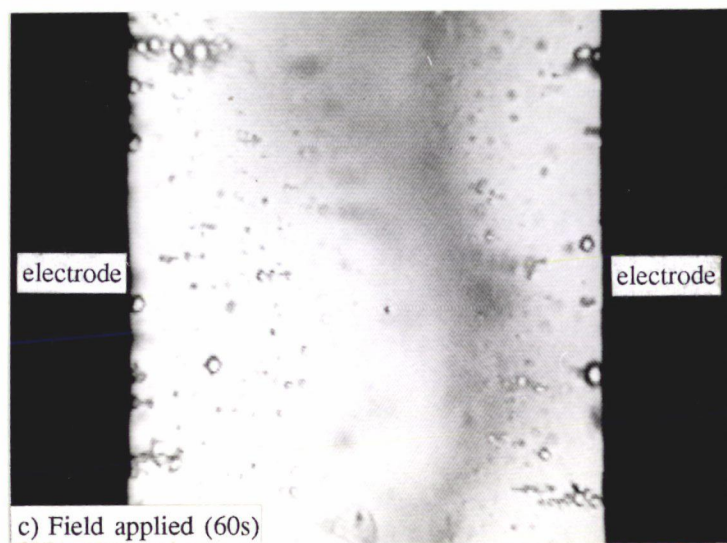
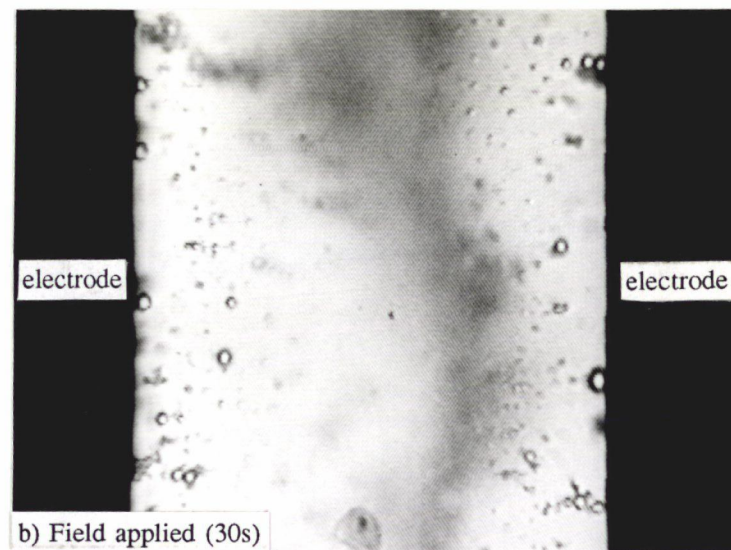
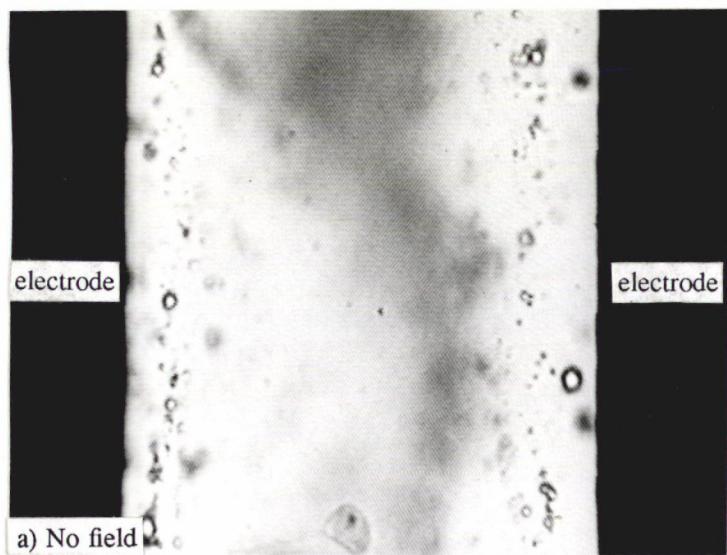


Figure 5.8. Chains of droplets collected at the electrodes.

Droplet collection in the regions of higher electric field intensities, may prove to be a useful phenomenon in phase separation. After collecting the dispersed droplets into an appropriate region, complete phase separation may be achieved by the following processes. The clean oil can be drawn out and the collected droplets can be removed from the electrodes periodically. Alternately, the collected droplets can be coalesced by the application of a single high voltage pulse or a series of high voltage pulses[51], followed by the removal of the coalesced droplets via sedimentation. In view of the possibility of using droplet collection as part of the processes involved in phase separation, further studies were carried out to elucidate the best frequency for droplet collection. The findings for such an investigation are discussed in the following section.

5.2. Part 2 : Optimum Frequency for Droplet Collection

The velocity spectra obtained for suspended water droplets of diameters $5.1\ \mu\text{m}$ and $4.25\ \mu\text{m}$, using the experimental procedures in section 4.3.1, are shown in Figure 5.9. For the purpose of comparison, part of the velocity spectra obtained for droplets of diameter $6.8\ \mu\text{m}$ is also shown in Figure 5.9. The spectrum obtained for $5.1\ \mu\text{m}$ droplets has a distinct peak at approximately 450 MHz. The data obtained for $4.25\ \mu\text{m}$ droplets, however, has a less pronounced maximum at the same frequency. This is due to the uncertainty associated with the present technique which will be discussed at the end of this section. Nevertheless, the peak at approximately 450 MHz is obvious from the additional data obtained for $6.8\ \mu\text{m}$ droplets. Figure 5.9

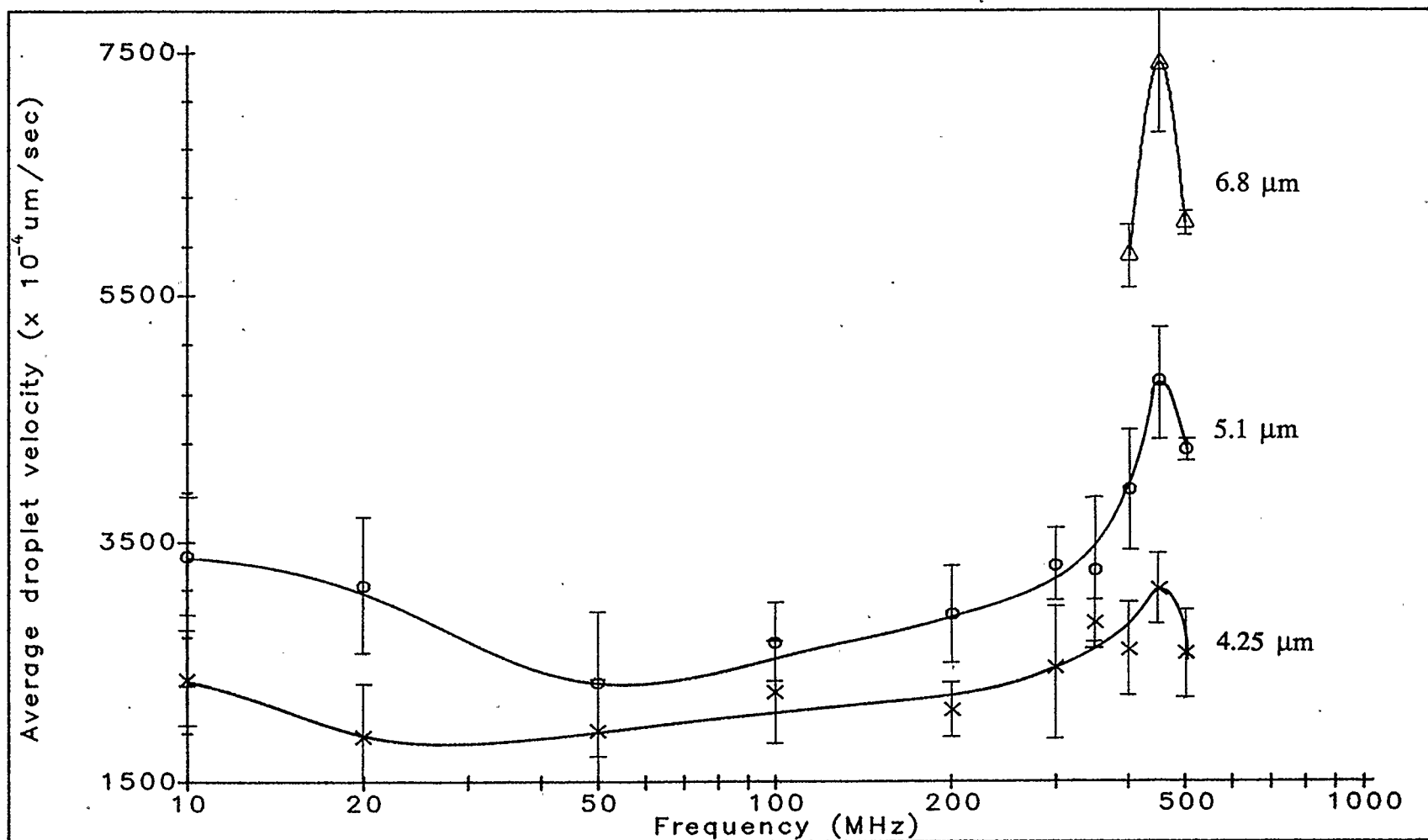


Figure 5.9. Velocity spectra of water droplets .

also indicates that the frequency at which this peak occurs is independent of the droplet size.

The data obtained for 5.1 μm droplets was normalized with respect to the maximum average velocity value and replotted in Figure 5.10 as normalized velocity versus frequency. The purpose is to show that the peak at 450 MHz is significant, since the droplet velocity at this frequency is higher than that at 50 MHz by a factor greater than two. Thus, it is concluded that the time required to collect the water droplets at 450 MHz is at least half the time required if the operating frequency is at 50 MHz.

The data obtained for the velocity spectra, as shown in Figure 5.9, suggests an additional lower frequency peak at around 10 MHz. The peaks in the velocity spectra are readily interpreted as the dielectric relaxation the emulsion system undergoes [26,27]. Several investigators have suggested various polarization relaxations that could assist in the interpretation of complex systems, such as aqueous dispersed systems. The polarization mechanisms most pertinent to the present analysis, in terms of the frequency range under study, are listed in Table 3.2. In order to assign the precise interpretation of the observed polarization relaxation, more velocity spectra must be obtained for the same frequency range but with different parameters (for example, with different ionic conductivity of the emulsion and volume fraction of the dispersed phase). For the present study, since the peak at approximately 450 MHz is independent of the droplet size and is in the frequency range of 1 MHz to 100 GHz, Table 3.2 suggests that the relaxation may be due to

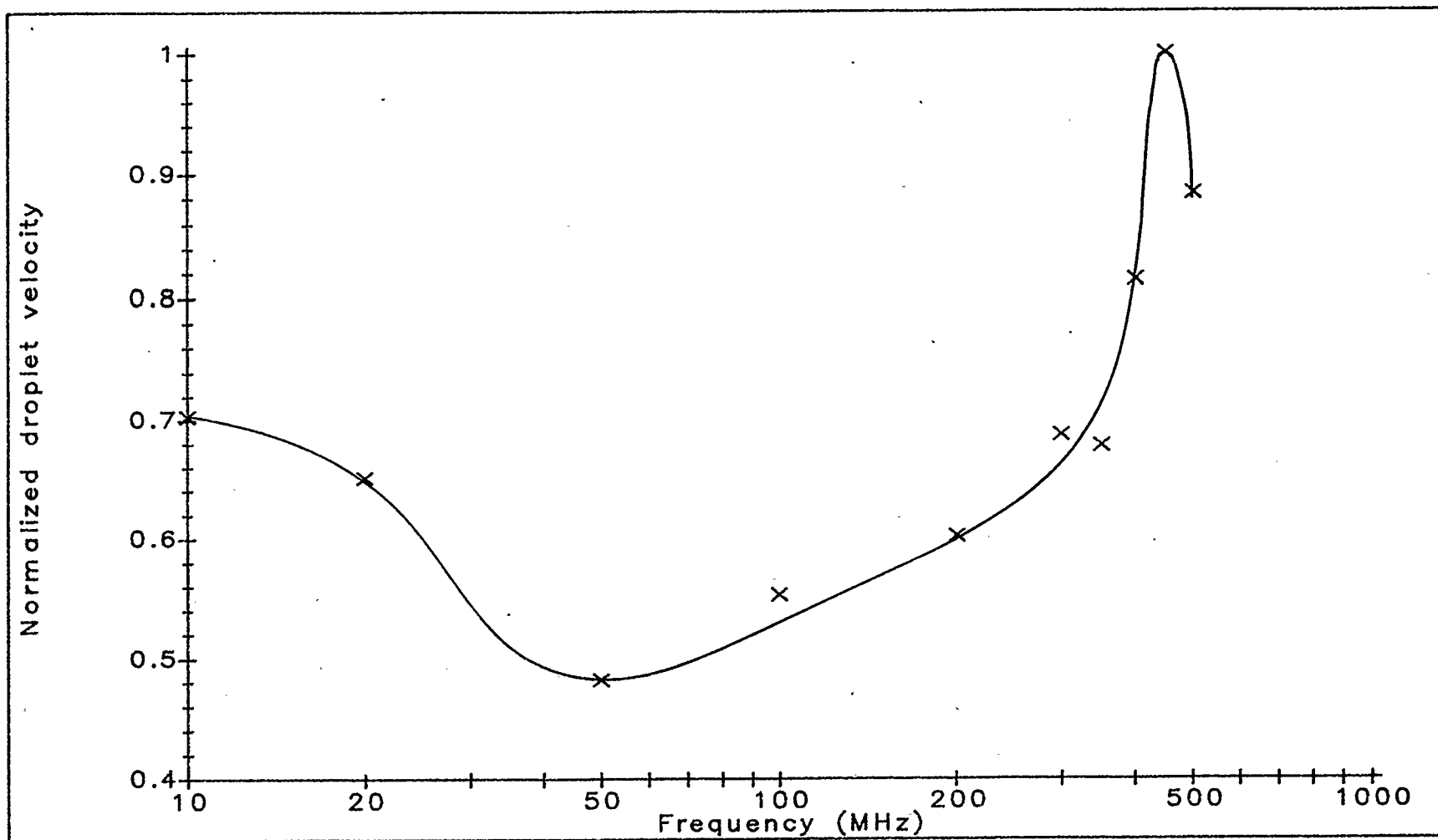


Figure 5.10. Normalised velocity spectrum of 5.1 μm water droplets.

dipolar orientation polarization. Dipolar polarization of water is known to relax at 20 GHz at room temperature [36], hence the observed relaxation cannot be due to dipolar polarization of "free" water. W/O emulsions from the oil-field are known to have asphaltenes and resins, polar components of crude oil, adsorbed at the droplet envelopes. The observed peak may be explained in terms of the relaxation of these polar crude components. Although Sayakhov has attributed the dispersion that he observed at 3 MHz to the relaxation of polar asphaltenes and resins, the possibility of asphaltenes and resins relaxing at 450 MHz is equally valid. This is because asphaltenes and resins are known to occur in various physical structures [52,53]. The peak at around 10 MHz, on the other hand, can possibly be due to Maxwell-Wagner polarization at the bulk interface or Schwarz type of counterion polarization since they relax in the frequency range of 100 kHz to 100 MHz. See Table 3.2.

The droplet velocities at 450 MHz can be calculated for different droplet sizes, if the velocity for one droplet size is known. This can be seen from equation (3.15), which is rewritten as

$$\vec{v} = \frac{1}{3} \frac{K_e}{\eta} \nabla |\vec{E}|^2 a^2 ,$$

where η and average $\nabla |\vec{E}|^2$ are constants in the present study. Hence, the average droplet velocity can be expressed as

$$|\vec{v}| = K_1 K_e a^2 \quad (5.1)$$

where K_1 is a constant. In addition, since the dielectric dispersion at 450 MHz is independent of droplet radius, the droplet velocity at this frequency can further be

simplified to

$$|\vec{v}| = Ca^2 \quad (5.2)$$

where C is a constant. Using equation (5.2) and the average droplet velocities obtained (from experiment) for the three droplet sizes, the average C calculated is 172. The droplet velocities for the three droplet sizes are then calculated using C , and are tabulated in Table 5.1. The measured droplet velocities for the droplets are also shown in Table 5.1 for comparison. The measured velocities of the droplets are found to be within 7% of the calculated values. Discrepancy between the two values may be attributed to the uncertainty in the present techniques and in the assumption that the average velocity obtained for the 5.1 μm droplets is a true value.

Size	Droplet velocity ($\times 10^{-4} \mu\text{m/sec}$)	
	measured	calculated
5.1 μm	4808	4474
4.25 μm	3099	3107
6.8 μm	7417	7953

Table 5.1. Measured and calculated average velocities at 450 MHz

The technique used for determining the velocity spectra is subjected to some criticism. First, it is time consuming to search for a single droplet of the desired size. Second, the data obtained is unable to provide a high degree of certainty. The major sources of uncertainty may include:

- 1) The inaccuracy in measuring the droplet size on the monitor screen using a circle template. The template used to measure the diameters of the droplets has a resolution of $0.28\mu\text{m}$. In this case, a droplet measured to be $5.1\mu\text{m}$ can be anywhere in the range $5.1\mu\text{m} \pm 0.28\mu\text{m}$. Similarly, a droplet measured to be $4.25\mu\text{m}$ can be anywhere in the range $4.25\mu\text{m} \pm 0.28\mu\text{m}$. However, the uncertainty associated with measuring a droplet of diameter $5.1\mu\text{m}$ is $\pm 5.6\%$ compared to $\pm 6.7\%$ for a droplet of diameter $4.25\mu\text{m}$. The higher uncertainty in measuring the diameter of $4.25\mu\text{m}$ droplets combined with the fact that the average droplet velocity is directly proportional to the square of the droplet radius may explain the difficulty in resolving the peak at about 450 MHz.
- 2) The distance between the two wire electrodes varies slightly after each wash. Data was obtained for electrode spacing of $0.165\text{ mm} \pm 3\%$.
- 3) The centre of the two electrodes is not always in the same horizontal plane.
- 4) The fluctuation in the room temperature at which all studies are carried out is assumed to be negligible.

Although the present technique is unable to provide a high degree of accuracy, nevertheless it is able to provide an approximate operating frequency for the optimum collection of water droplets in an w/o emulsion.

CHAPTER 6

CONCLUSIONS AND RECOMMENDATIONS

Suspended water droplets are found to collect at the electrodes, in the form of "pearl chains", when the water-in-oil (w/o) emulsion is exposed to a non-uniform electric field in the frequency range 10 MHz to 500 MHz. The optimum frequency for such a collection, within this range, is found to be at approximately 450 MHz. Other physical effects are also observable throughout this frequency range. Aggregate particles first orientate with their long axis parallel to the electric field line, followed by movement towards the higher field intensity region. Mutual attractions between the neighbouring droplets eventually lead to "pearl chain" formation. Droplet coalescence is also possible due to mutual attraction, but in the present studies "pearl chain" formation is the more dominant effect observed.

The phenomenon of droplet collection at the electrodes is a positive indication of the possibility of using high frequency electromagnetic fields (where the electric field is non-uniform) for phase separation. A knowledge of the optimum frequency for droplet collection at the electrodes will be invaluable in the design of electrostatic separators. However, the practicality of such separation on a large scale has yet to be determined.

Recommendations for further work are :

- 1) The maximum field strength that can be applied before droplet re-emulsification occurs needs to be determined.
- 2) The relationship between the rate of droplet collection and the field strength should be investigated.
- 3) The use of a series of high voltage pulses or a single high voltage pulse to induce droplet coalescence (collected droplets) should be investigated.
- 4) The overall physical design of a separator which will incorporate the collection phenomenon and a method for the removal of the collected water droplets should be investigated. Some of the points to be taken into consideration include the physical arrangement of the electrodes, the input flow rate of the emulsion and the output flow rate of the clean oil. Such studies are needed to evaluate the practicality of such a design on a large scale basis.

REFERENCES

1. D. R. Skinner, *Introduction To Petroleum Production*, Gulf Publishing Company, Houston (1982).
2. HTI Hydrotek, *Private communication*: 1986 .
3. L. C. Waterman, "Coalescence: electrical coalescers," *Chemical Engineering Progress* **61**(10) pp. 51-57 (Oct. 1965).
4. P.J. Bailes and S.K.L. Larkai, "Liquid phase separation in pulsed d.c fields," *Transaction of Institute of Chemical Engineer* **60** pp. 115-121 (1982).
5. A. N. Stepanenko and V. V. Papko, "Investigation of the conductivity of emulsions of the water-in-oil type in high-strength electric fields," *Colloids Journal of the USSR* **44**(4) pp. 720-723 (July-Aug. 1982). Translated from *Kolloidnyi Zhurnal*
6. A. A. Yunusov, G. A. Babalyan, and G. M. Akhmadiev, "Effects of surface-active demulsifiers on electrical conductivity of emulsions of water in crude oil," *Chemistry and Technology of Fuel and Oil* **19**(7-8) pp. 351-353 (Jul.-Aug. 1983).
7. G. M. Panchenkov and V. M. Vinogradov, "Water-in-oil emulsion in a constant homogeneous electric field," *Chemistry and Technology of Fuel and Oil* **15** (5-6) pp. 438-441 (May-Jun. 1970).

8. G. M. Panchenkov, V. V. Papko, and L. K. Tsabek, "Effect of frequency of an external electrical field on the coalescence of aqueous drops in an emulsion of the 'water in oil' type," *Chemistry and Technology of Fuel and Oil*, (11-12) pp. 803-805 (Nov.-Dec. 1969).
9. V. M. Vinogradov, A. N. Stepanenko, and V. V. Papko, "Equation for motion of water drops of hydrocarbon emulsion in a direct-current field," *Chemistry and Technology of Fuels and Oil* 20(7-8) pp. 377-379 (Jul.-Aug. 1984).
10. Charles D. Hendricks and Shafik E. Sadek, "Electric field enhanced coalescence of drops in liquid emulsions," *IEEE Transactions on Industry Applications* IA-13 (5) pp. 489-493 (Sept./Oct. 1977).
11. Shafik E. Sadek and Charles D. Hendricks, "Electrical coalescence of water droplets in low-conductivity oils," *Industrial Engineering Chemical Fundamental* 13(2) pp. 139-142 (1974).
12. T. J. Williams and A. G. Bailey, "Changes in the size distribution of a water-in-oil emulsion due to electric field induced coalescence," *Industry Application Society, IEEE-IAS annual meeting*, pp. 1162-1166 (1984).
13. Donald R. Burris, "Dual polarity oil dehydration," *Petroleum Engineer International*, pp. 30-41 (Aug. 1977).
14. Herman P. Schwan, "EM-field induced force effects," pp. 371-389 in *Interactions Between Electromagnetic Fields and Cells*, ed. H.P. Schwan, Plenum Press, New York (1985).

15. T.J. Williams and A.G. Bailey, "The resolution times of water-in-oil emulsions subjected to external electric fields," *The sixth Conference on Electrostatic Phenomena*, pp. 39-44 (1983). The Institute of Physics, Bristol and London
16. G.A. Babalyan and M. Kh. Akhmadeev, "Breaking emulsions by an electric field in presence of demulsifiers," *Doklady Chemical Technology* **205-207** pp. 186-188 (Jul.-Dec. 1972). Translation from Doklady Akademii Nauk SSSR
17. Herbert A. Pohl, *Dielectrophoresis*, Cambridge University Press (1978).
18. Herbert A. Pohl and J. Kent Pollock, "Biological dielectrophoresis," pp. 329-376 in *Modern Bioelectrochemistry*, ed. Hendrik Keyzer, Plenum Press, New York (1982).
19. A. A. Teixeira-Pinto, L. L. Nejelski, Jr, and J. L. Cutler, "The behaviour of unicellular organisms in an electromagnetic field," *Experimental Cell Research*, (20) pp. 548-564 (1960).
20. I. J. Lin, "General conditions for dielectrophoretic and magnetohydrostatic levitation," *Journal of Electrostatics* **15** pp. 53-65 (1984).
21. Herbert A. Pohl and Joe S. Crane, "Dielectrophoresis of cells," *Biophysical Journal* **11** pp. 711-727 (1971).
22. F. M. Joos, R. W. L. Snaddon, and N. A. Johnson, "Electrostatic droplet growth in a neutrally bouyant emulsion," *Industry Application Society, IEEE-IAS annual meeting*, pp. 1156-1161 (1984).

23. H. P. Schwan and Lawrence D. Sher, "Alternating-current field-induced forces and their biological implications," *Journal of Electrochemistry Society : Reviews and news* **116**(1) pp. 22c-26c (Jan. 1969).
24. Friedrich A. Sauer, "Interaction-forces between microscopic particles in an external electromagnetic field," pp. 181-202 in *Interactions Between Electromagnetic Fields and Cells*, ed. H. P. Schwan, Plenum Press, New York (1985).
25. Friedrich A. Sauer, "Forces on suspended particles in the electromagnetic field," pp. 134-144 in *Coherent Excitations in Biological Systems*, ed. F. Kremer, Springer-Verlag Berlin Heidelberg, Germany (1983).
26. F.L. Sayakhov and V.S. Khakimov, "Features of the behaviour of water-oil emulsion in high frequency electromagnetic field," *Electrochemistry in Industrial Processing and Biology*, (4) pp. 55-60 (1984).
27. F. L. Sayakhov and V. S. Khakimov, "Treatment of water-oil emulsion by H.F. and U.H.F. electric fields," *Electrochemistry in Industrial Process and Biology*, (6) pp. 72-74 (1978).
28. R. M. Bashirova, F. L. Sayakhov, and V. S. Khakimov, "Effect of high-frequency fields on the stability of water-in-oil emulsions," *Chemistry and Technology of Fuel and Oil* **19**(1-2) pp. 84-85 (Jan.-Feb. 1983).
29. Arthur Rose, *The Condensed Chemical Dictionary*, Reinhold Publishing Corporation, New York (1966).

30. Philip Sherman, *Emulsion Science*, Academic Press Inc. Ltd., London (1968).
31. Paul Becher, *Emulsion: Theory and Practice*, Robert E. Krieger Publishing Company, Florida (1966).
32. Abubakr S. Bahaj and Adrian G. Bailey, "The relationship between dielectrophoretic and impedance response of dielectric particles immersed in aqueous media," *IEEE Transaction on Industry Applications* 21(5) pp. 1300-1305 (Sept.-Oct. 1985).
33. R. S. Allan and S. G. Mason, "Effects of electric fields on coalescence in liquid+liquid systems," *Transactions of Faraday Society* 57 pp. 2027-2040 (Mar. 1961).
34. Duncan J. Shaw, *Introduction To Colloid And Surface Chemistry*, Butterworth & Co. Ltd., London (1980). Third edition
35. Samuel Y. Liao, *Microwave Devices and Circuit*, Prentice-Hall, Englewood Cliffs, New Jersey (1980).
36. Maria A. Stuchly, "Fundamentals of the interactions of radio-frequency and microwave energies with matter," pp. 75-93 in *Biological Effects and Dosimetry of Nonionizing Radiation*, ed. Sol M. Michaelson, Plenum Press, New York (1983).
37. Dr-Ing. Carl Heck, *Magnetic Materials and Their Applications*, Butterworth & Co. Ltd., London (1979).

38. Richard Gerber and Robert R. Birss, *High Gradient Magnetic Separation*, John Wiley & Sons Ltd., Great Britain (1983).
39. Julius Adams Stratton, *Electromagnetic Theory*, McGraw Hill, New York (1941).
40. R. Von Hippel, *Dielectric Materials And Applications*, The Technology Press of M.I.T. and John Wiley & Sons, New York (1954).
41. Andrzej Kraszewski, "Microwave aquametry," *Polish Academy of Sciences* 39 pp. 48-58 (1981).
42. R.J. Adamson, "A continuous automated system," *MSc. Thesis*, Electrical Engineering Department, University of Calgary, (Apr. 1986).
43. Karan Kaler, *Private communication*. 1986.
44. A. Chelkowski, *Dielectric Physics*, Elsevier Scientific Publishing Company, Amsterdam (1980).
45. S. S. Dukhin and V. N. Shilov, *Dielectric phenomena and the double layer in disperse systems and polyelectrolytes*, John Wiley and Sons (1974).
46. B.J. Carroll, "The stability of emulsions and mechanisms of emulsion breakdown," in *Surface and Colloid Science*, ed. Egon Matijevic, John Wiley & Sons, New York (1976).
47. L. Benguigui and I. J. Lin, "More about the dielectrophoretic force," *Journal of Applied Physics* 53(2) pp. 1141-1143 (Feb. 1982).

48. L. Petrakis and P. F. Ahner, "Use of high gradient magnetic separation techniques for the removal of oil and solids from water effluents," *IEEE Transactions on Magnetics* **12**(5) pp. 486-488 (Sep 1956).
49. Ross E. Robertson and Yves Flottat, *Mechanism of demulsification of heavy oil w/o emulsions promoted by a non-ionic surfactant*, University of Calgary, Department of Chemistry (1984).
50. E. Kuffel and W.S. Zaengl, *High Voltage Engineering*, Pergamon Press, Oxford (1984).
51. U. Zimmermann, "Electric field-mediated fusion and related electrical phenomena," *Biochimica et Biophysica Acta*, (694) pp. 227-277 (1982).
52. James G. Speight and S.E. Moschopedis, "On the molecular nature of petroleum asphaltenes," pp. 1-15 in *Chemistry of Asphaltenes*, ed. N.C. Li, American Chemical Society (1981).
53. T.F. Yen, "The role of asphaltene in heavy crudes and tar sands," *Proc. 1st. Int. Conf. on The Future of Heavy Crude and Tar Sands*, pp. 174-179 (Jun. 1979).